بنام ایزد توانا

بیوشیمی۲ (متابولیسم)

استاد: دکتر امیر آراسته

جلسه اول: مقدمه و کنترل متابولیسم

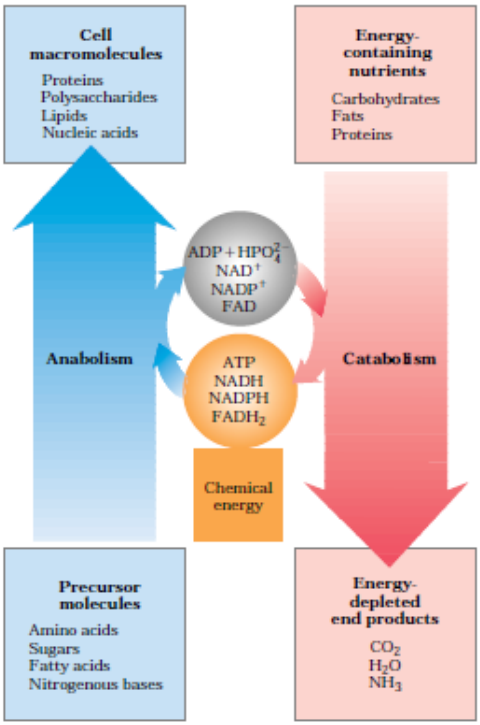


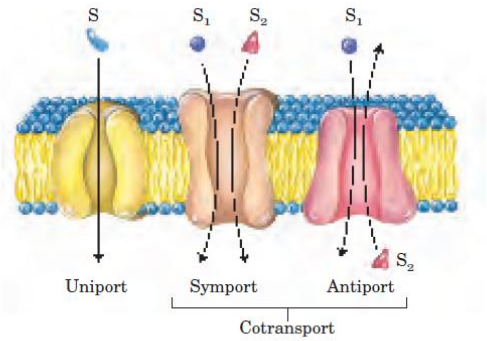


**FIGURE 11–34** **Three general classes of transport systems.** Transporters differ in the number of solutes (substrates) transported and the direction in which each is transported. Examples of all three types of transporters are discussed in the text. Note that this classification tells us nothing about whether these are energy-requiring (active transport) or energy-independent (passive transport) processes.

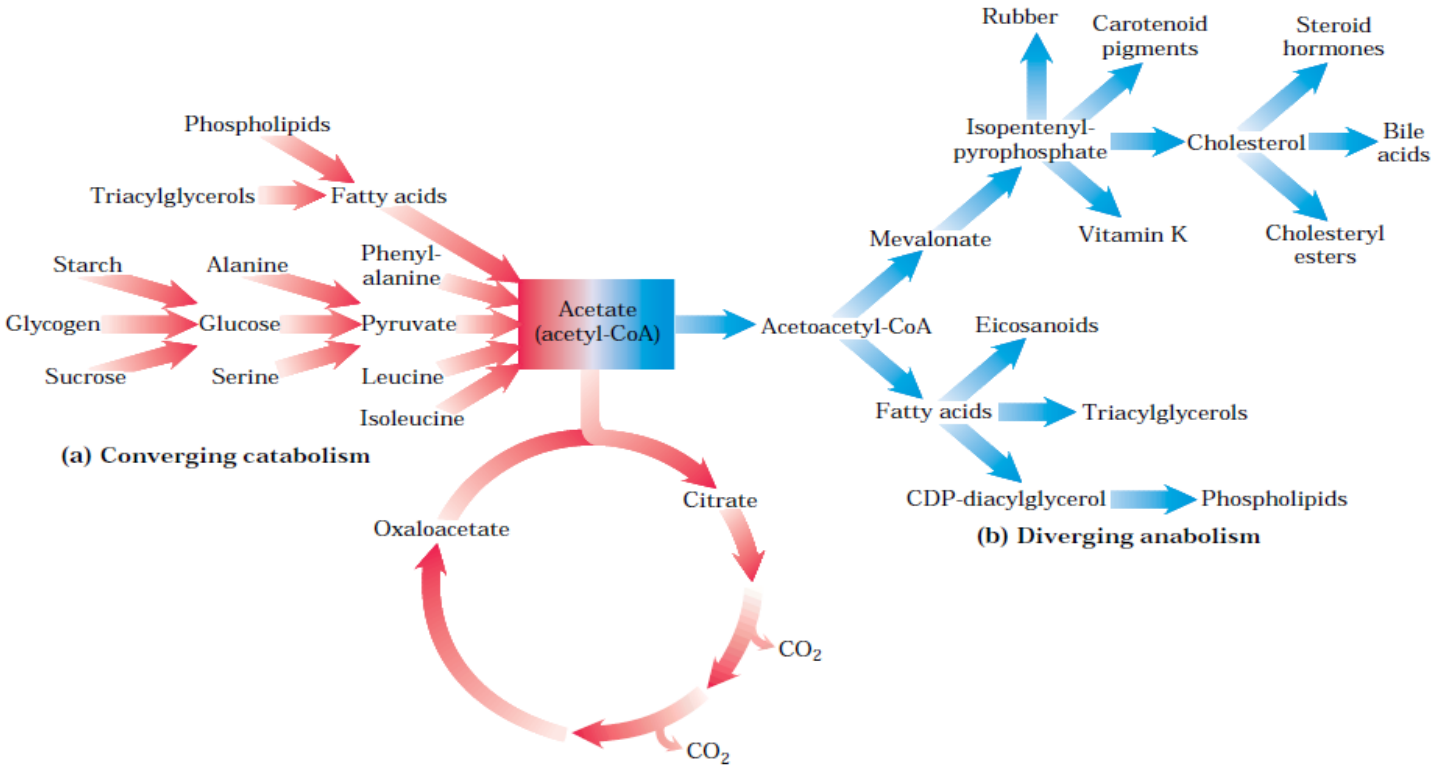

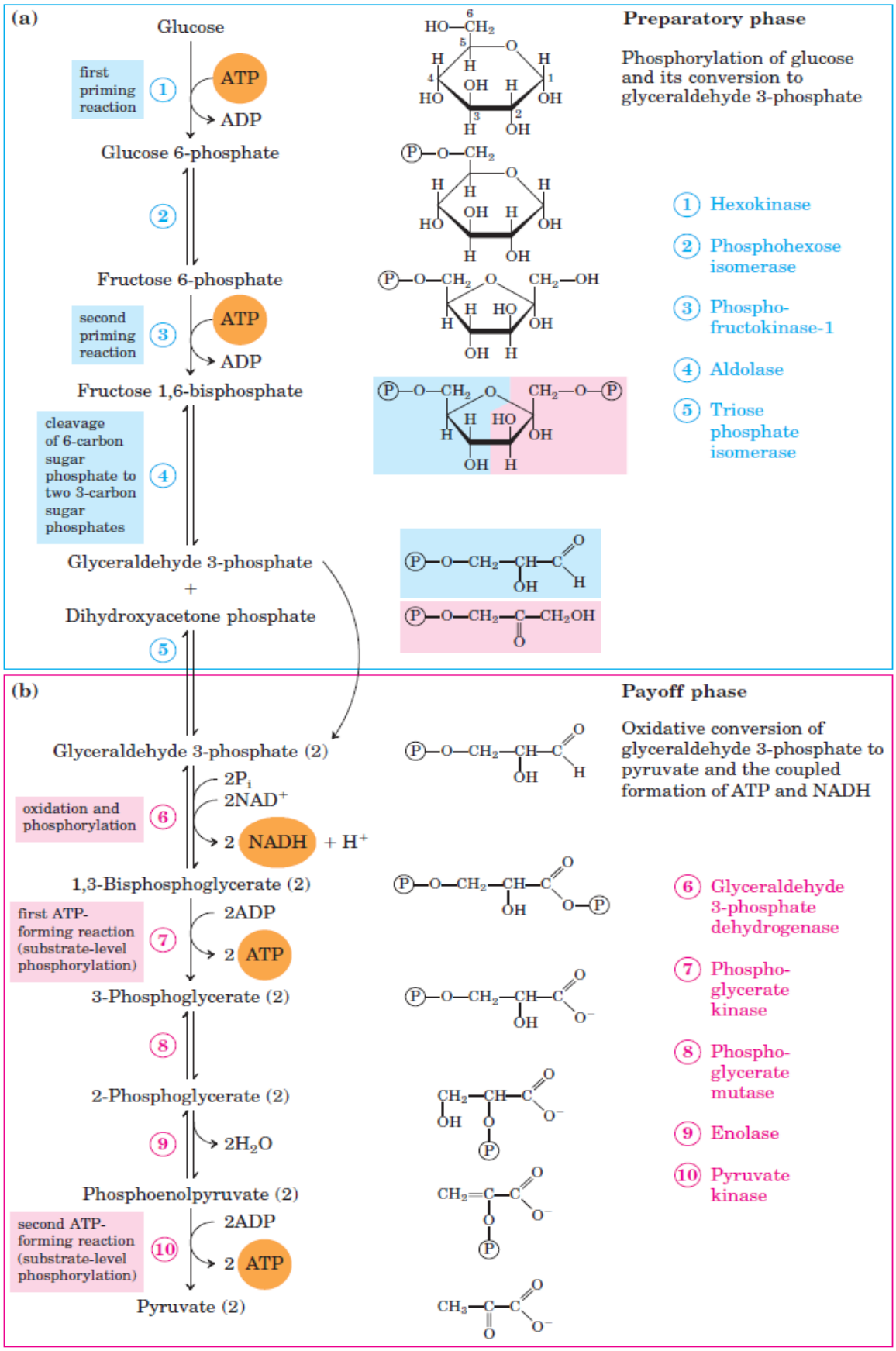
(a)
Glucose
first priming reaction
1
ATP
ADP
Glucose 6-phosphate
2
Fructose 6-phosphate
second priming reaction
3
ATP
ADP
Fructose 1,6-bisphosphate
cleavage of 6-carbon sugar phosphate to two 3-carbon sugar phosphates
4
Glyceraldehyde 3-phosphate
+
Dihydroxyacetone phosphate
5
Preparatory phase
Phosphorylation of glucose and its conversion to glyceraldehyde 3-phosphate
1 Hexokinase
2 Phosphohexose isomerase
3 Phospho-fructokinase-1
4 Aldolase
5 Triose phosphate isomerase
(b)
Glyceraldehyde 3-phosphate (2)
oxidation and phosphorylation
6
2Pi
2NAD+
2 NADH + H+
1,3-Bisphosphoglycerate (2)
first ATP-forming reaction (substrate-level phosphorylation)
7
2ADP
2 ATP
3-Phosphoglycerate (2)
8
2-Phosphoglycerate (2)
9
2H2O
Phosphoenolpyruvate (2)
second ATP-forming reaction (substrate-level phosphorylation)
10
2ADP
2 ATP
Pyruvate (2)
Payoff phase
Oxidative conversion of glyceraldehyde 3-phosphate to pyruvate and the coupled formation of ATP and NADH
6 Glyceraldehyde 3-phosphate dehydrogenase
7 Phospho-glycerate kinase
8 Phospho-glycerate mutase
9 Enolase
10 Pyruvate kinase

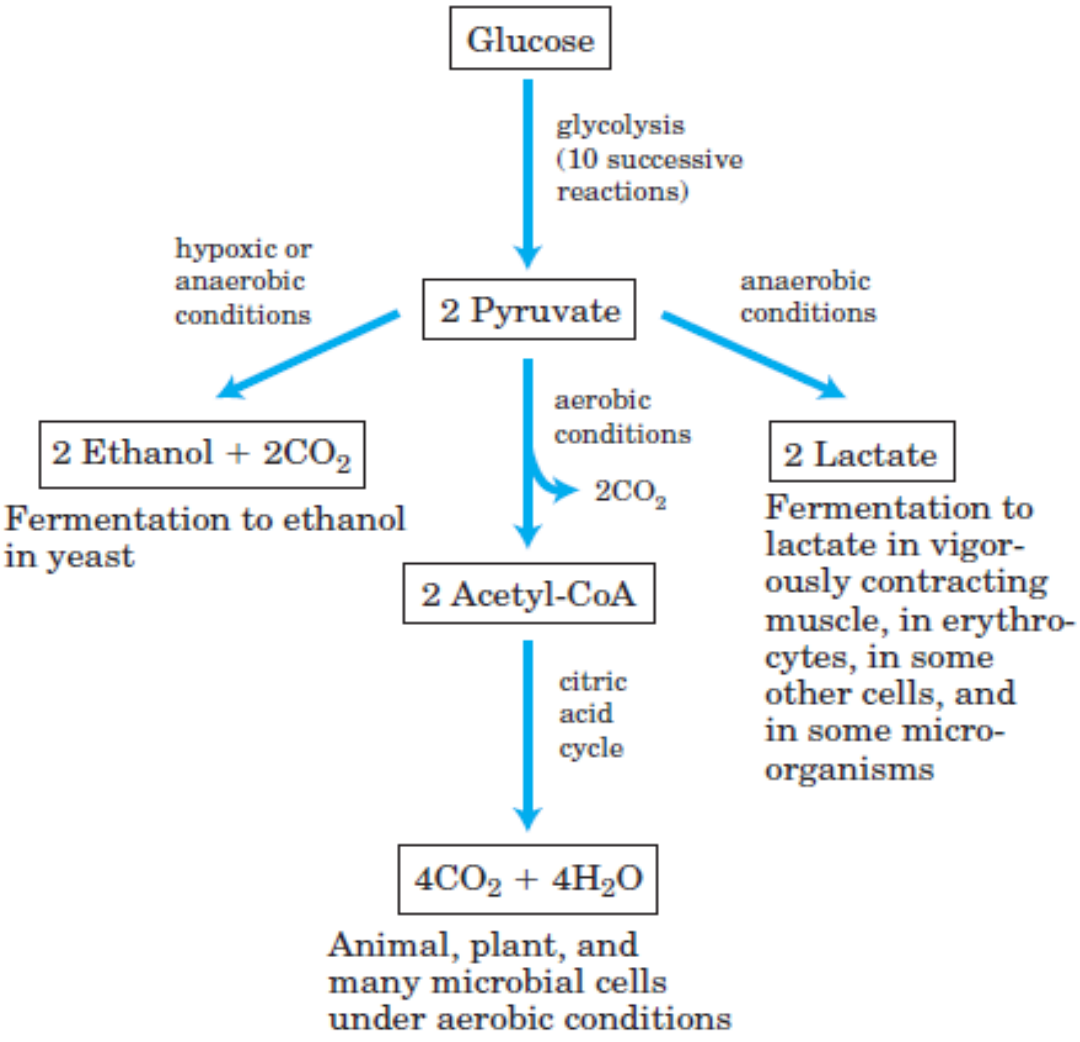


**FIGURE 14–3 Three possible catabolic fates of the pyruvate formed in glycolysis.** Pyruvate also serves as a precursor in many anabolic reactions, not shown here.

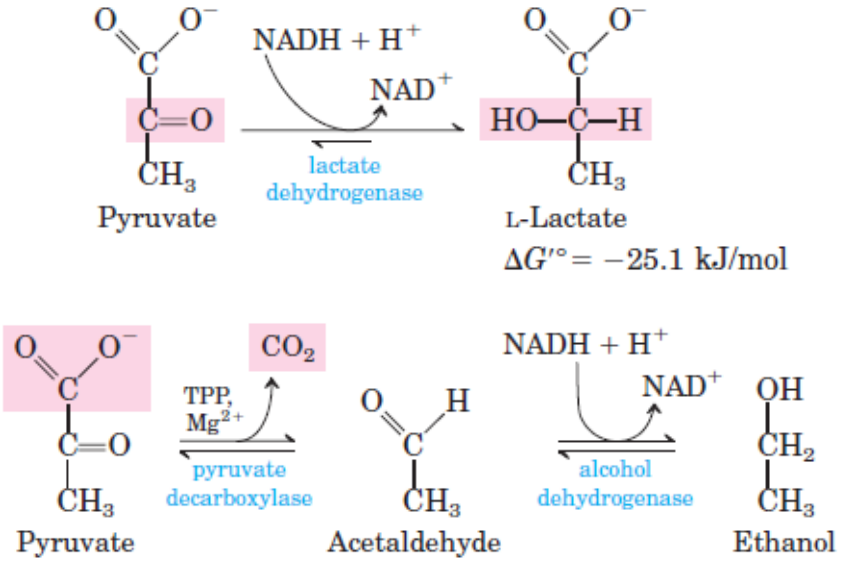

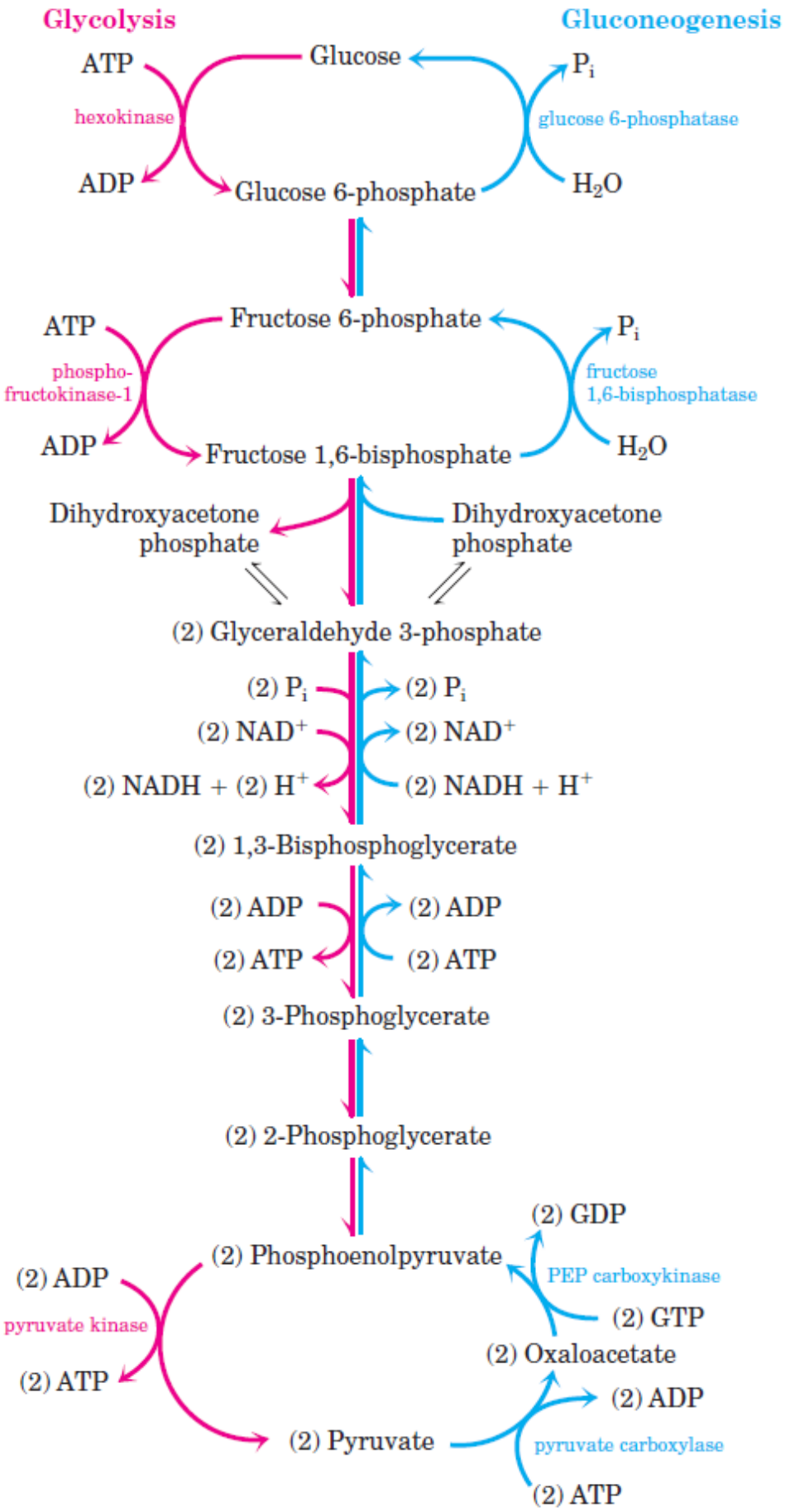
Glycolysis
Gluconeogenesis
ATP
Glucose
$P_i$
hexokinase
glucose 6-phosphatase
ADP
Glucose 6-phosphate
$H_2O$
ATP
Fructose 6-phosphate
$P_i$
phospho-
fructokinase-1
fructose
1,6-bisphosphatase
ADP
Fructose 1,6-bisphosphate
$H_2O$
Dihydroxyacetone
phosphate
Dihydroxyacetone
phosphate
(2) Glyceraldehyde 3-phosphate
(2) $P_i$
(2) $P_i$
(2) $NAD^+$
(2) $NAD^+$
(2) NADH + (2) $H^+$
(2) NADH + $H^+$
(2) 1,3-Bisphosphoglycerate
(2) ADP
(2) ADP
(2) ATP
(2) ATP
(2) 3-Phosphoglycerate
(2) 2-Phosphoglycerate
(2) GDP
(2) Phosphoenolpyruvate
PEP carboxykinase
(2) ADP
(2) GTP
pyruvate kinase
(2) Oxaloacetate
(2) ATP
(2) ADP
(2) Pyruvate
pyruvate carboxylase
(2) ATP

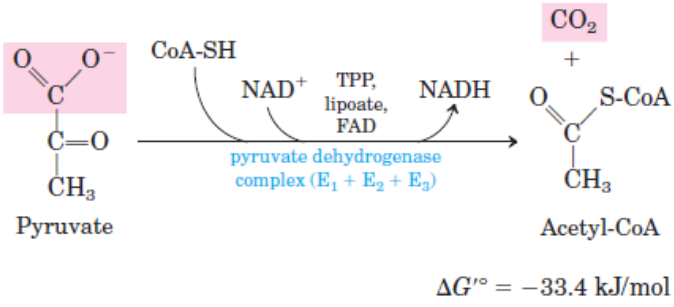


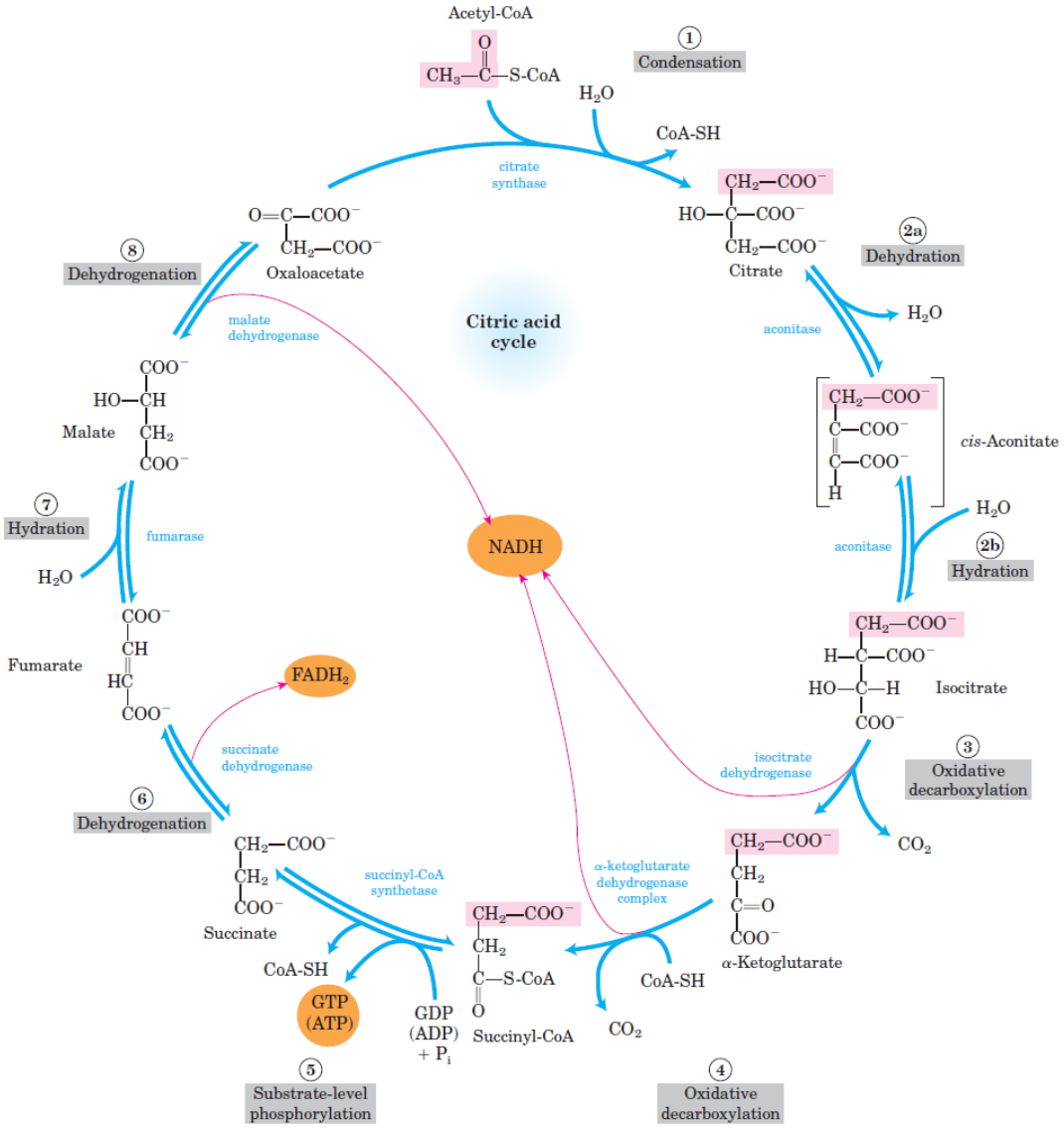


**FIGURE 16–7 Reactions of the citric acid cycle.** The carbon atoms shaded in pink are those derived from the acetate of acetyl-CoA in the first turn of the cycle; these are *not* the carbons released as $CO_2$ in the first turn. Note that in succinate and fumarate, the two-carbon group derived from acetate can no longer be specifically denoted; because succinate and fumarate are symmetric molecules, C-1 and C-2 are indistinguishable from C-4 and C-3. The number beside each reaction step corresponds to a numbered heading on pages 608–612. The red arrows show where energy is conserved by electron transfer to FAD or $NAD^+$, forming $FADH_2$ or NADH + $H^+$. Steps ①, ③, and ④ are essentially irreversible in the cell; all other steps are reversible. The product of step ⑤ may be either ATP or GTP, depending on which succinyl-CoA synthetase isozyme is the catalyst.

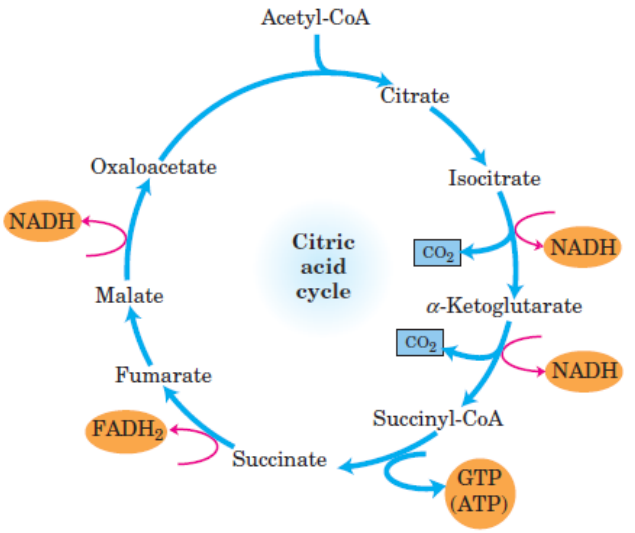


**FIGURE 16–13** **Products of one turn of the citric acid cycle.** At each turn of the cycle, three NADH, one $FADH_2$, one GTP (or ATP), and two $CO_2$ are released in oxidative decarboxylation reactions. Here and in several following figures, all cycle reactions are shown as proceeding in one direction only, but keep in mind that most of the reactions are reversible (see Fig. 16–7).

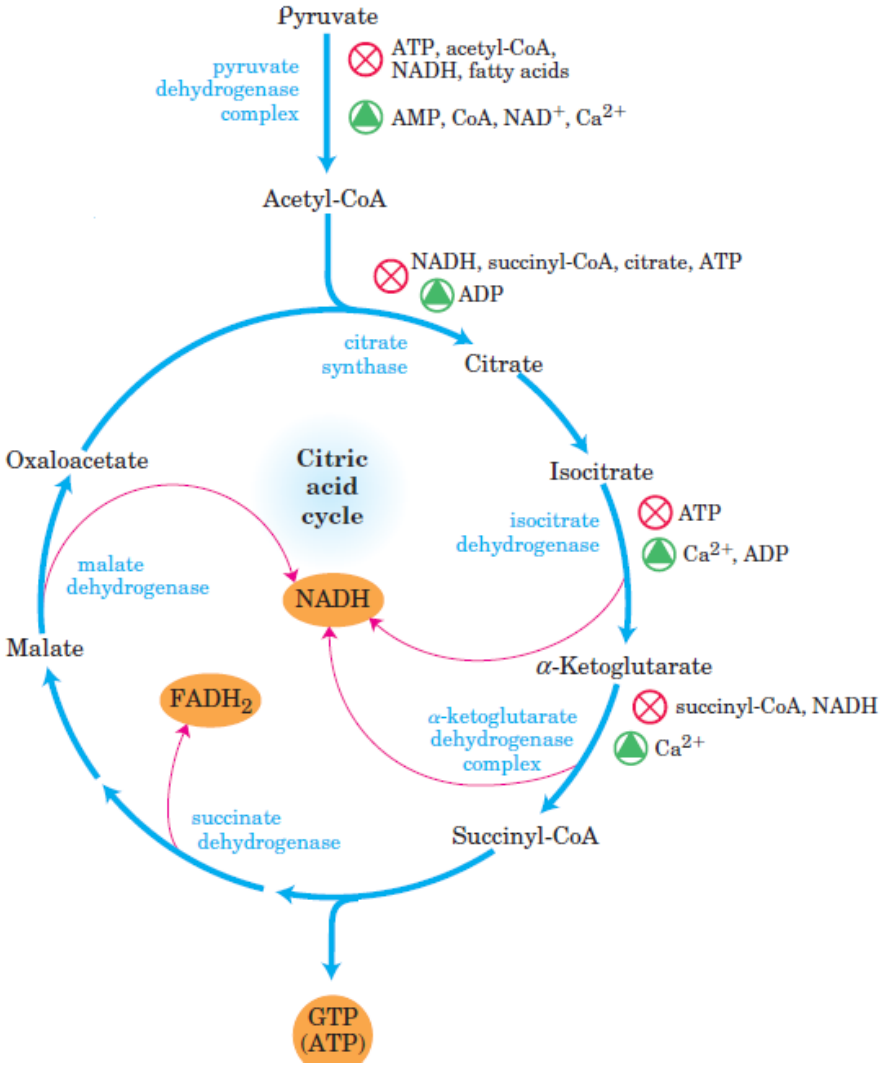

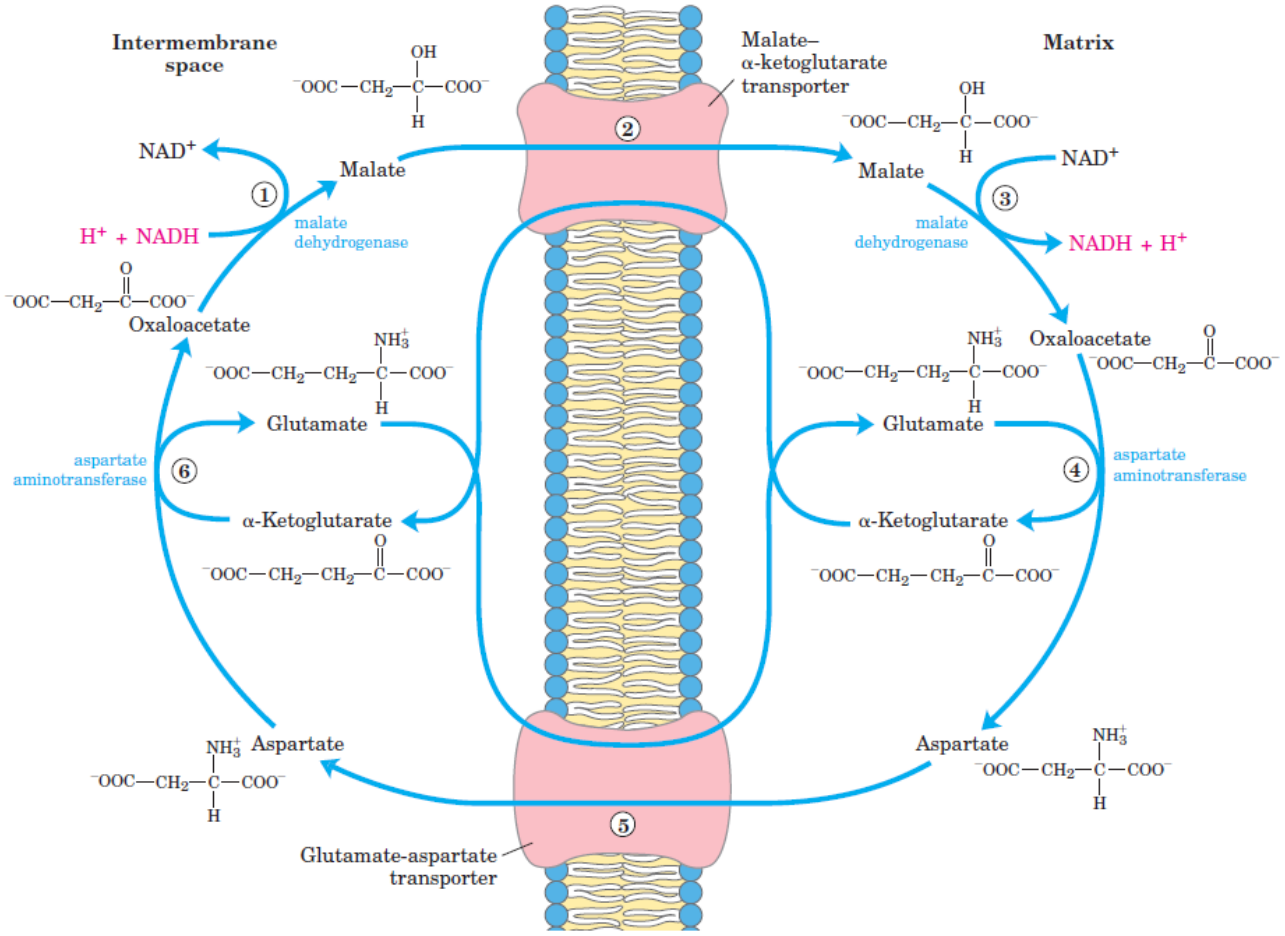


**FIGURE 19–27 Malate-aspartate shuttle.** This shuttle for transporting reducing equivalents from cytosolic NADH into the mitochondrial matrix is used in liver, kidney, and heart. (1) NADH in the cytosol (intermembrane space) passes two reducing equivalents to oxaloacetate, producing malate. (2) Malate crosses the inner membrane via the malate–α-ketoglutarate transporter. (3) In the matrix, malate passes two reducing equivalents to $NAD^+$, and the resulting NADH is oxidized by the respiratory chain. The oxaloacetate formed from malate cannot pass directly into the cytosol. (4) It is first transaminated to aspartate, which (5) can leave via the glutamate-aspartate transporter. (6) Oxaloacetate is regenerated in the cytosol, completing the cycle.

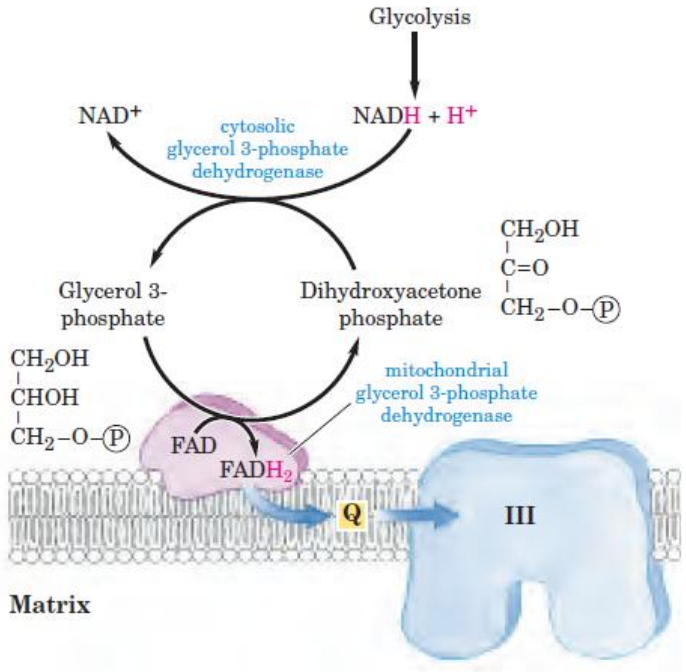


**FIGURE 19–28 Glycerol 3-phosphate shuttle.** This alternative means of moving reducing equivalents from the cytosol to the mitochondrial matrix operates in skeletal muscle and the brain. In the cytosol, dihydroxyacetone phosphate accepts two reducing equivalents from NADH in a reaction catalyzed by cytosolic glycerol 3-phosphate dehydrogenase. An isozyme of glycerol 3-phosphate dehydrogenase bound to the outer face of the inner membrane then transfers two reducing equivalents from glycerol 3-phosphate in the intermembrane space to ubiquinone. Note that this shuttle does not involve membrane transport systems.

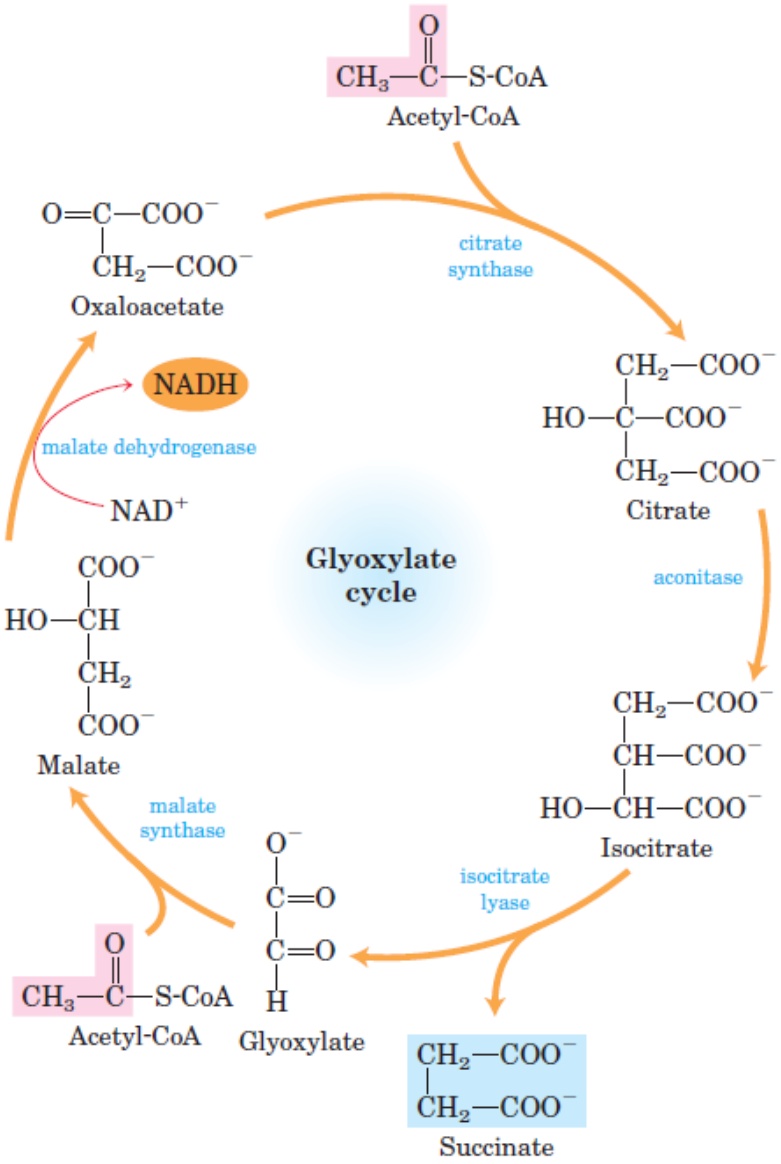


**FIGURE 16–20** **Glyoxylate cycle.** The citrate synthase, aconitase, and malate dehydrogenase of the glyoxylate cycle are isozymes of the citric acid cycle enzymes; isocitrate lyase and malate synthase are unique to the glyoxylate cycle. Notice that two acetyl groups (pink) enter the cycle and four carbons leave as succinate (blue). The glyoxylate cycle was elucidated by Hans Kornberg and Neil Madsen in the laboratory of Hans Krebs.

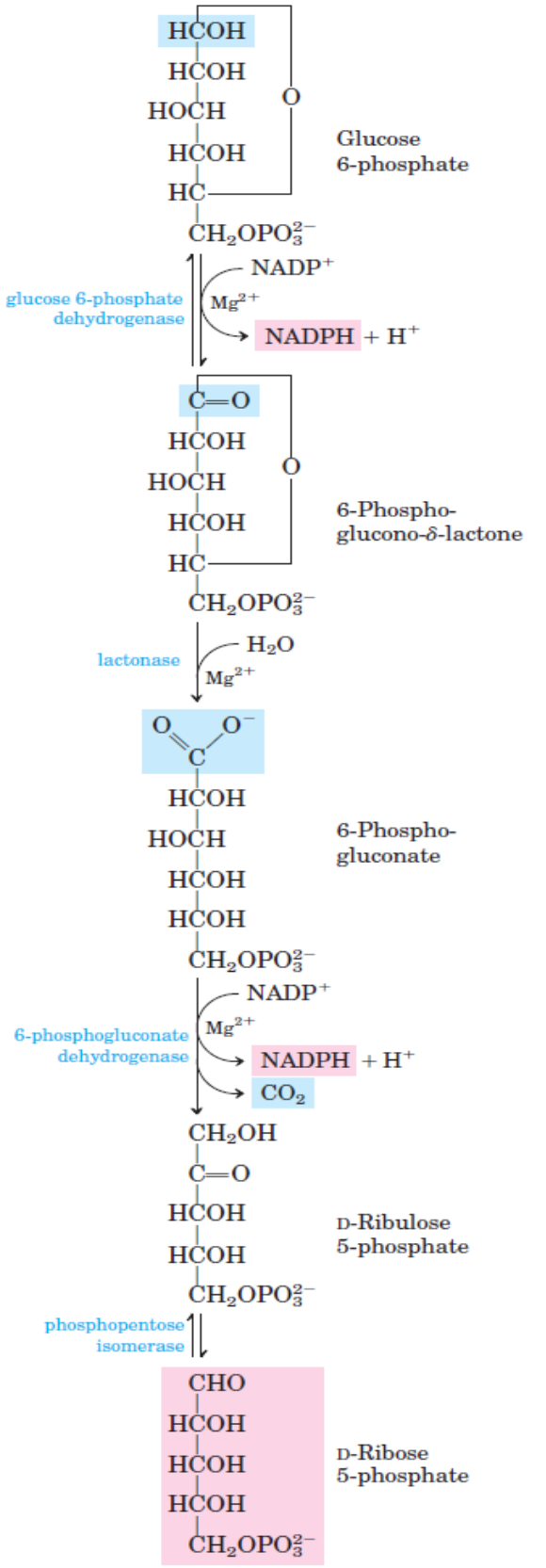


**FIGURE 14–21** **Oxidative reactions of the pentose phosphate pathway.** The end products are ribose 5-phosphate, $CO_2$, and NADPH.

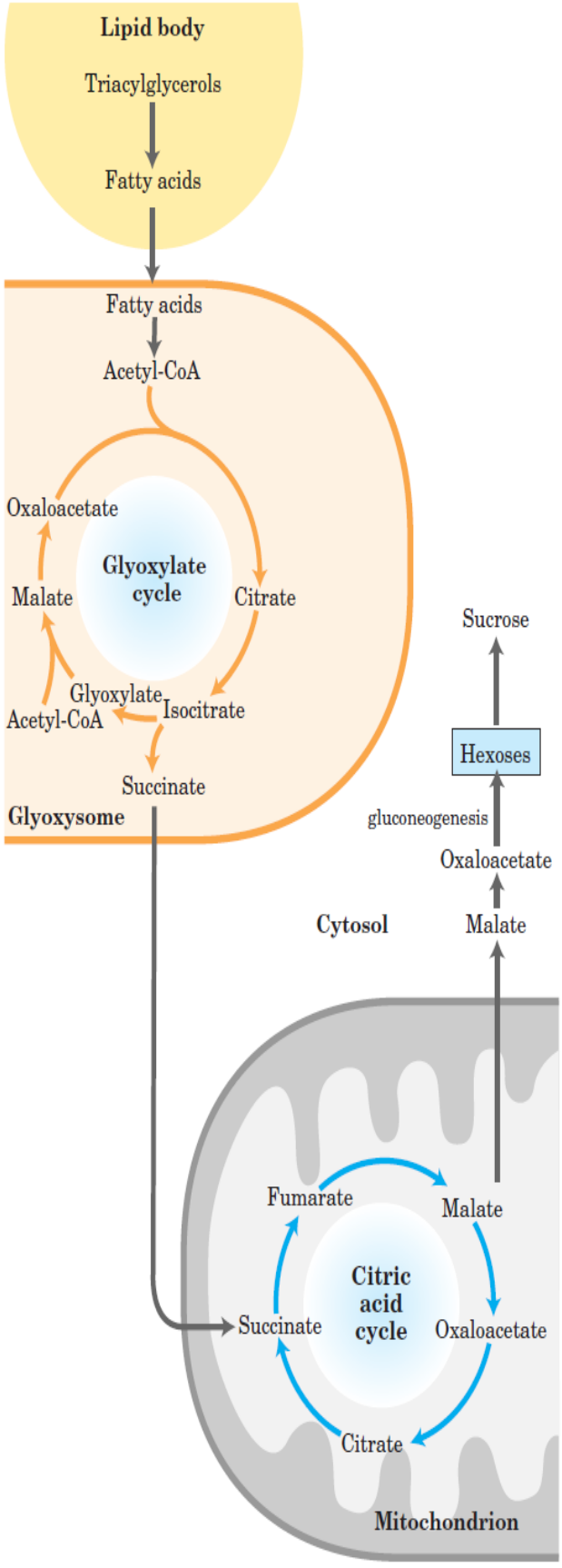


**FIGURE 16-22** Relationship between the glyoxylate and citric acid cycles. The reactions of the glyoxylate cycle (in glyoxysomes) proceed

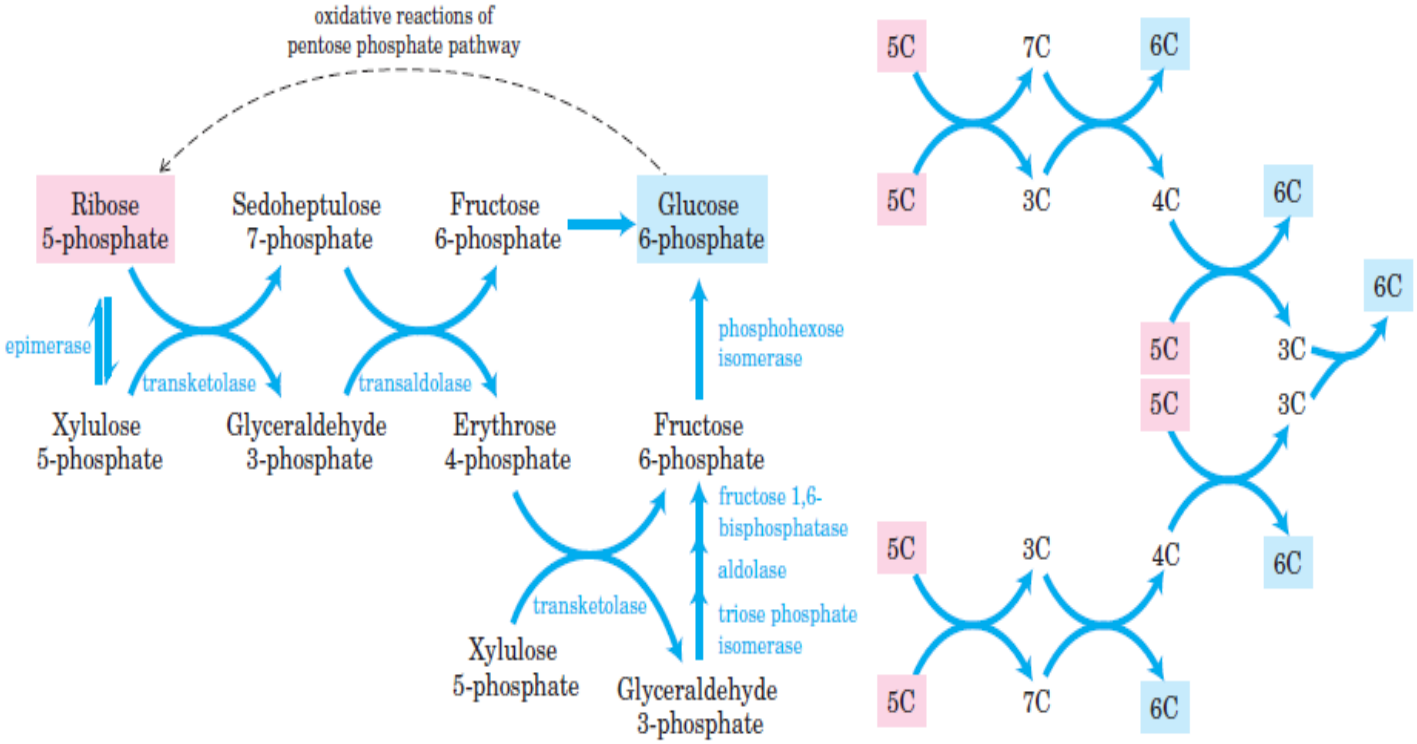


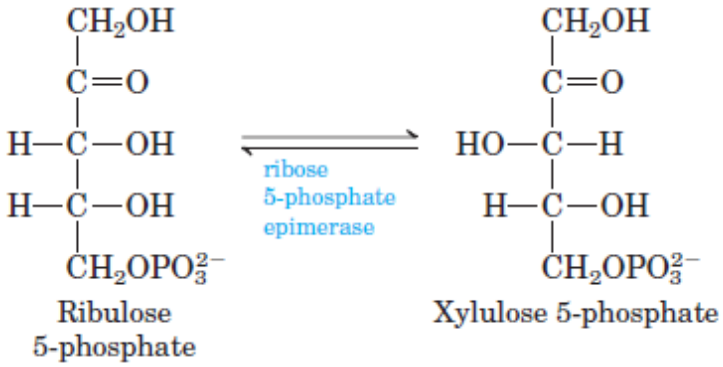


Ribulose 5-phosphate

Xylulose 5-phosphate

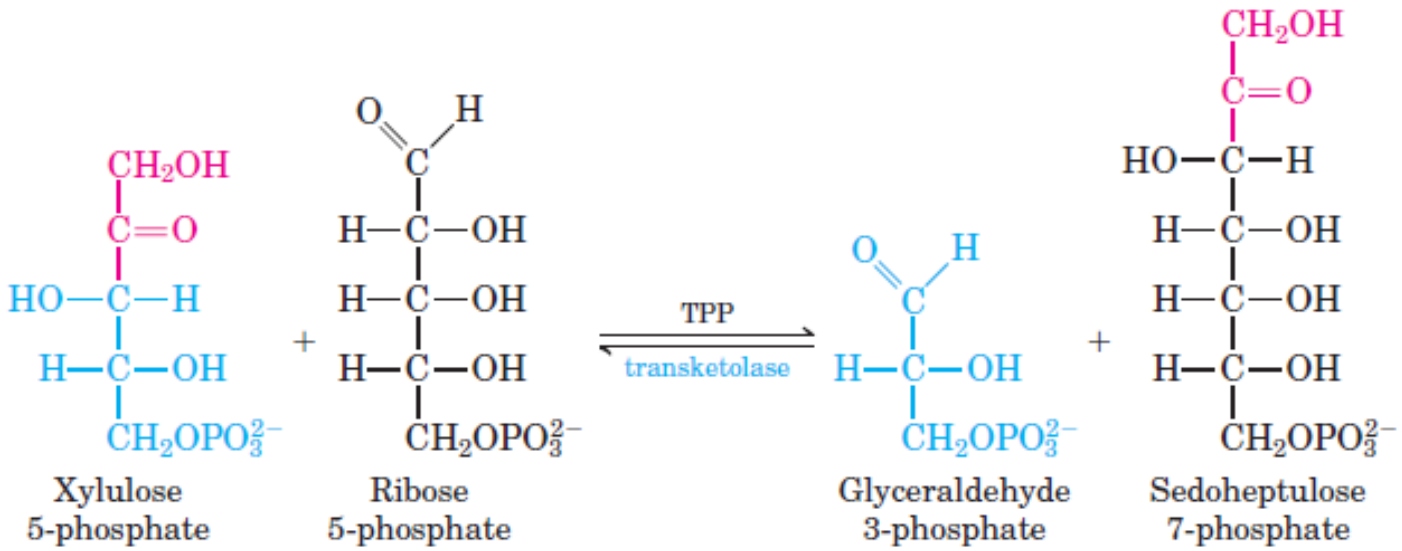


Xylulose 5-phosphate + Ribose 5-phosphate ⇌ Glyceraldehyde 3-phosphate + Sedoheptulose 7-phosphate

**FIGURE 15–3** **Removal of a terminal glucose residue from the nonreducing end of a glycogen chain by glycogen phosphorylase.** This process is repetitive; the enzyme removes successive glucose residues until it reaches the fourth glucose unit from a branch point (see Fig. 15–4).

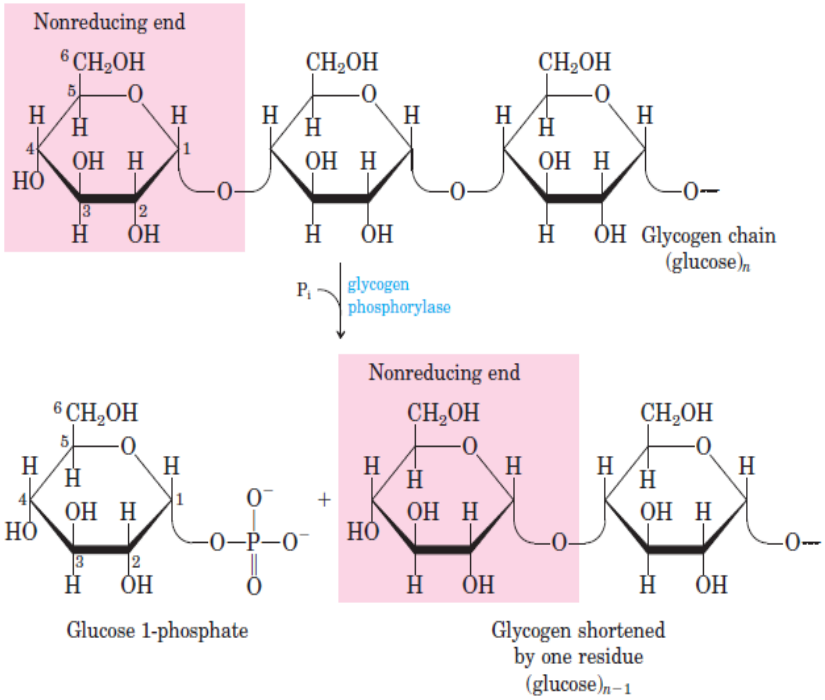


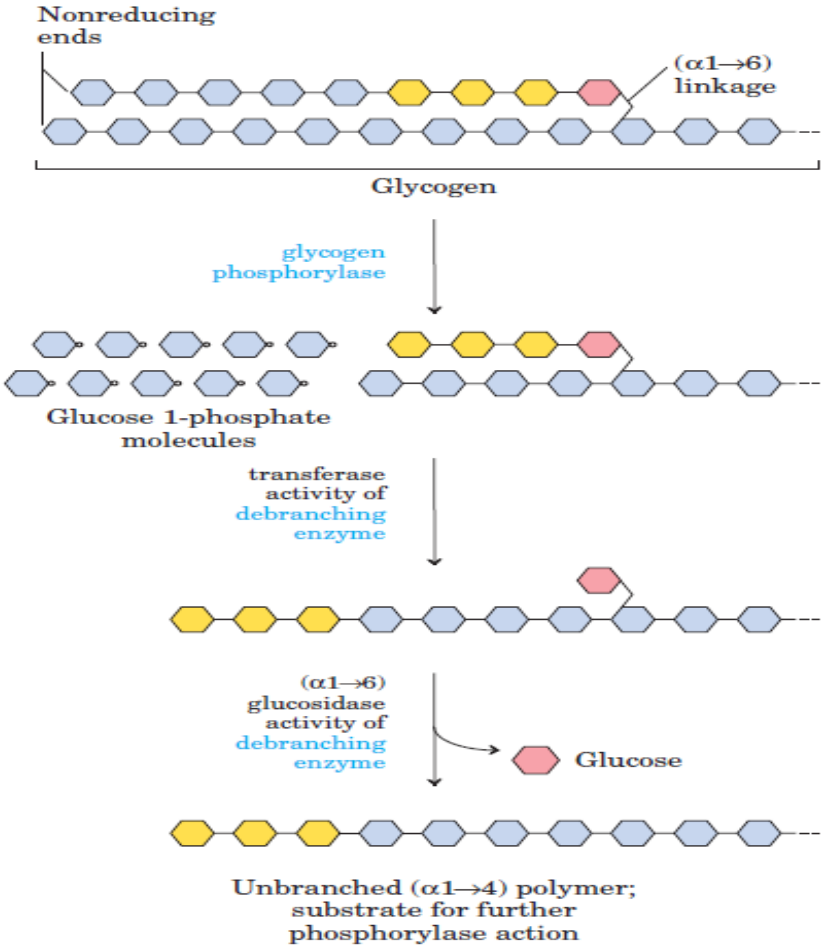

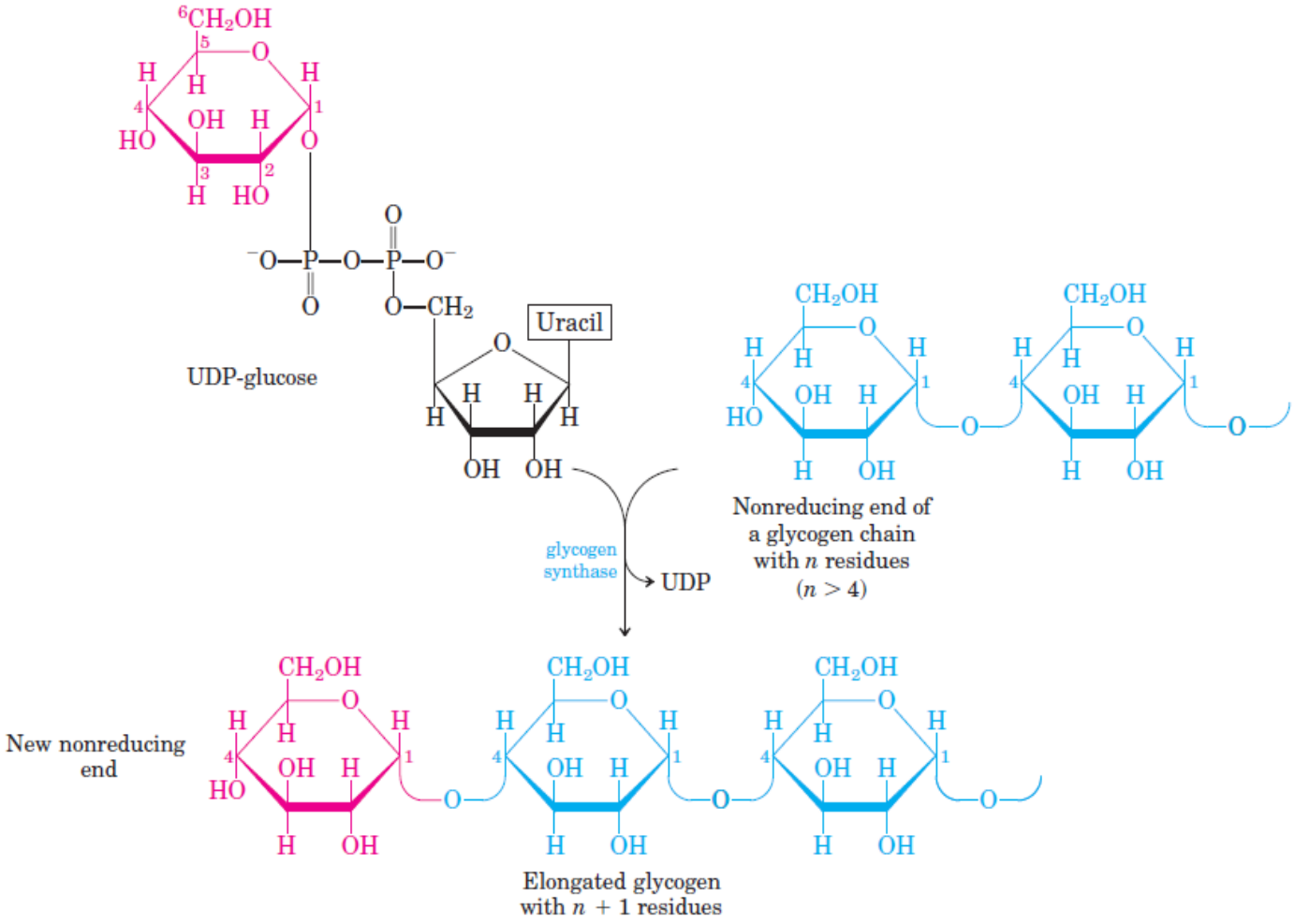


**FIGURE 15–8 Glycogen synthesis.** A glycogen chain is elongated by glycogen synthase. The enzyme transfers the glucose residue of UDP-glucose to the nonreducing end of a glycogen branch (see Fig. 7–15) to make a new ($\alpha$1→4) linkage.

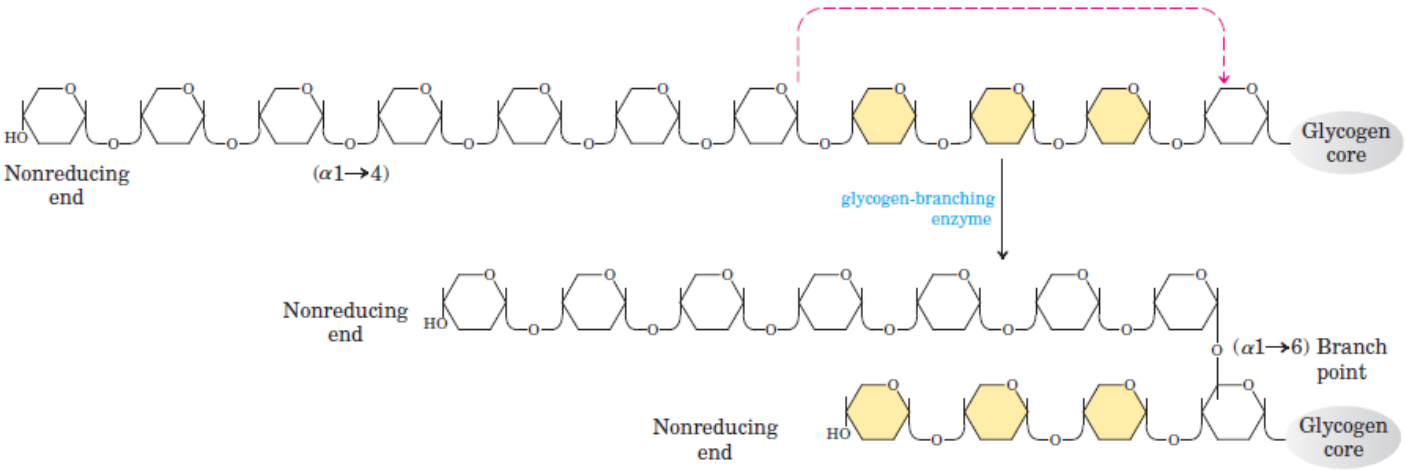


**FIGURE 15–9 Branch synthesis in glycogen.** The glycogen-branching enzyme (also called amylo (1→4) to (1→6) transglycosylase or glycosyl-(4→6)-transferase) forms a new branch point during glycogen synthesis.

**TABLE 19-3** The Protein Components of the Mitochondrial Electron-Transfer Chain

| Enzyme complex/protein | Mass (kDa) | Number of subunits* | Prosthetic group(s) |
|---|---|---|---|
| I NADH dehydrogenase | 850 | 43 (14) | FMN, Fe-S |
| II Succinate dehydrogenase | 140 | 4 | FAD, Fe-S |
| III Ubiquinone cytochrome *c* oxidoreductase | 250 | 11 | Hemes, Fe-S |
| Cytochrome *c*† | 13 | 1 | Heme |
| IV Cytochrome oxidase | 160 | 13 (3-4) | Hemes; $Cu_A$, $Cu_B$ |

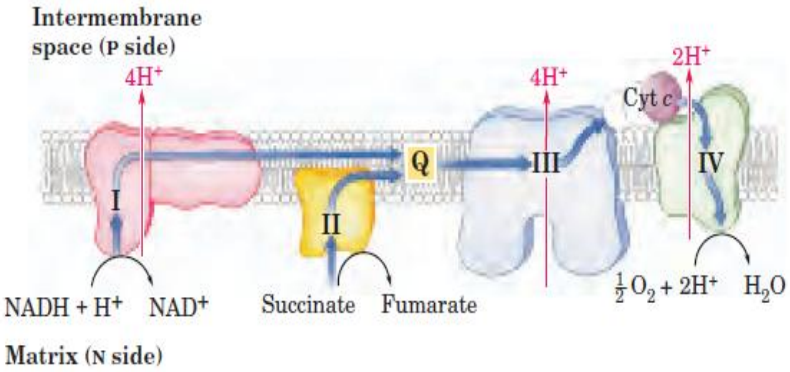


**FIGURE 19-15 Summary of the flow of electrons and protons through the four complexes of the respiratory chain.** Electrons reach Q through Complexes I and II. $QH_2$ serves as a mobile carrier of electrons and protons. It passes electrons to Complex III, which passes them to another mobile connecting link, cytochrome *c*. Complex IV then transfers electrons from reduced cytochrome *c* to $O_2$. Electron flow through Complexes I, III, and IV is accompanied by proton flow from the matrix to the intermembrane space. Recall that electrons from $\beta$ oxidation of fatty acids can also enter the respiratory chain through Q (see Fig. 19–8).

**TABLE 19-4** Agents That Interfere with Oxidative Phosphorylation or Photophosphorylation

| Type of interference | Compound* | Target/mode of action |
|---|---|---|
| Inhibition of electron transfer | Cyanide, Carbon monoxide | Inhibit cytochrome oxidase |
| | Antimycin A | Blocks electron transfer from cytochrome *b* to cytochrome $c_1$ |
| | Myxothiazol, Rotenone, Amytal, Piericidin A | Prevent electron transfer from Fe-S center to ubiquinone |
| | DCMU | Competes with $Q_B$ for binding site in PSII |
| Inhibition of ATP synthase | Aurovertin | Inhibits $F_1$ |
| | Oligomycin, Venturicidin | Inhibit $F_o$ and $CF_o$ |
| | DCCD | Blocks proton flow through $F_o$ and $CF_o$ |
| Uncoupling of phosphorylation from electron transfer | FCCP, DNP | Hydrophobic proton carriers |
| | Valinomycin | $K^+$ ionophore |
| | Thermogenin | In brown fat, forms proton-conducting pores in inner mitochondrial membrane |
| Inhibition of ATP-ADP exchange | Atractyloside | Inhibits adenine nucleotide translocase |

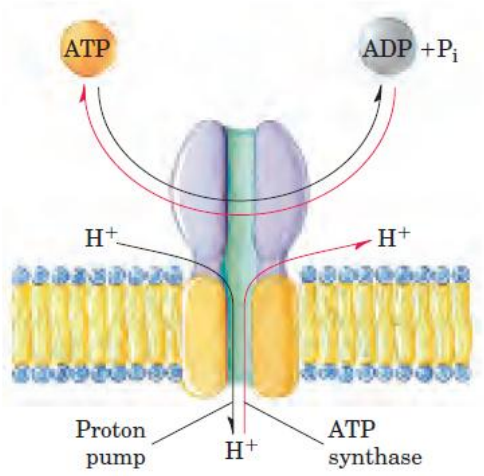


**FIGURE 11-40** **Reversibility of F-type ATPases.** An ATP-driven proton transporter also can catalyze ATP synthesis (red arrows) as protons flow *down* their electrochemical gradient. This is the central reaction in the processes of oxidative phosphorylation and photophosphorylation, both described in detail in Chapter 19.

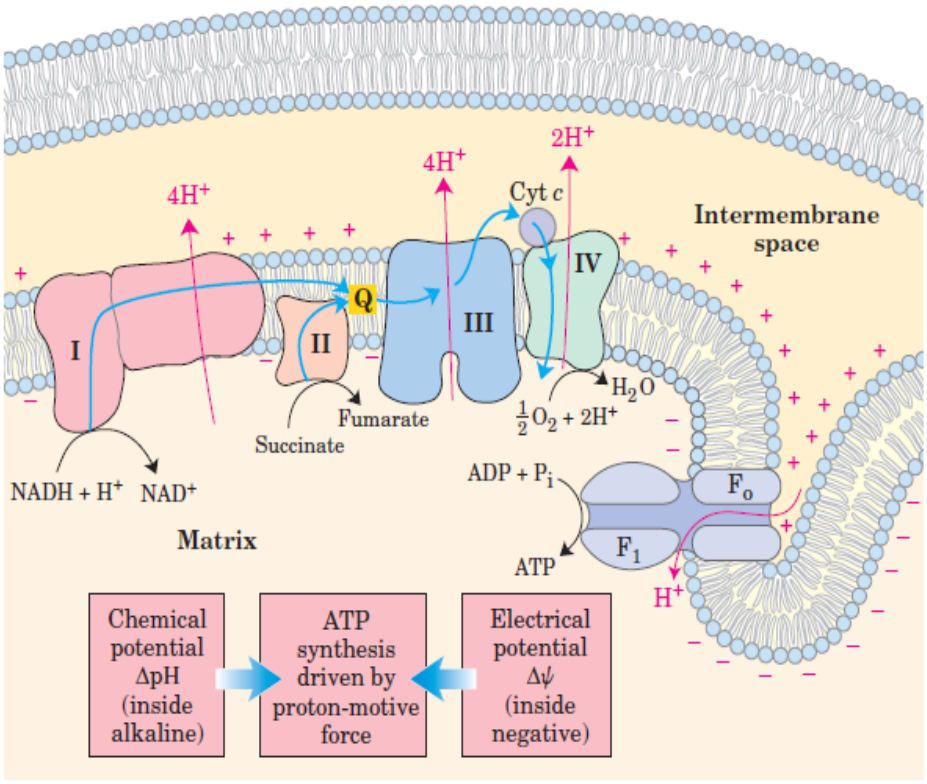


**FIGURE 19-17** **Chemiosmotic model.** In this simple representation of the chemiosmotic theory applied to mitochondria, electrons from NADH and other oxidizable substrates pass through a chain of carriers arranged asymmetrically in the inner membrane. Electron flow is accompanied by proton transfer across the membrane, producing both a chemical gradient (ΔpH) and an electrical gradient ($\Delta\psi$). The inner mitochondrial membrane is impermeable to protons; protons can reenter the matrix only through proton-specific channels ($F_o$). The proton-motive force that drives protons back into the matrix provides the energy for ATP synthesis, catalyzed by the $F_1$ complex associated with $F_o$.

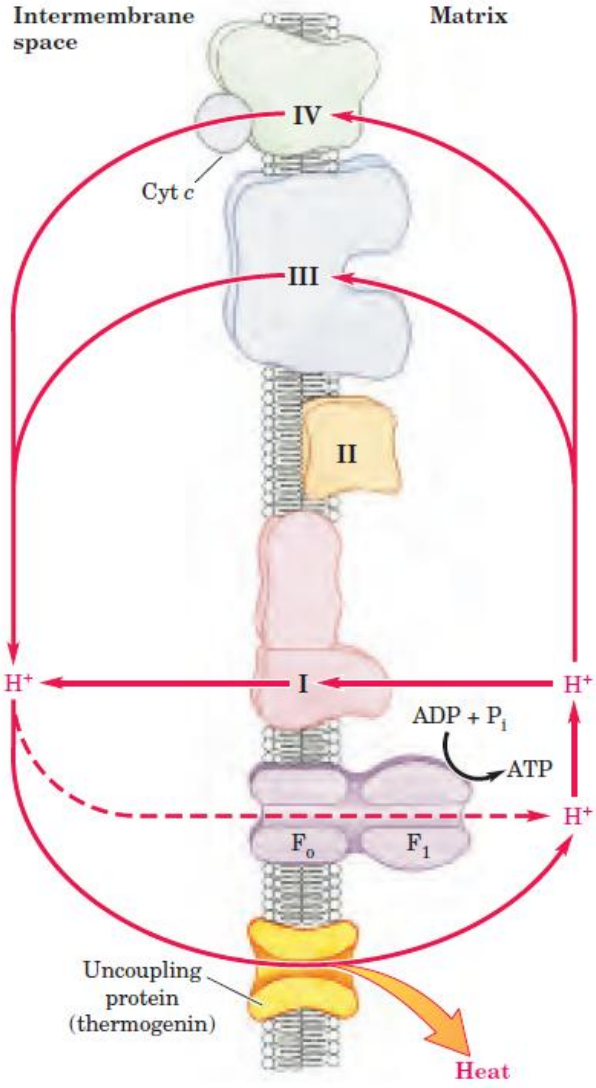


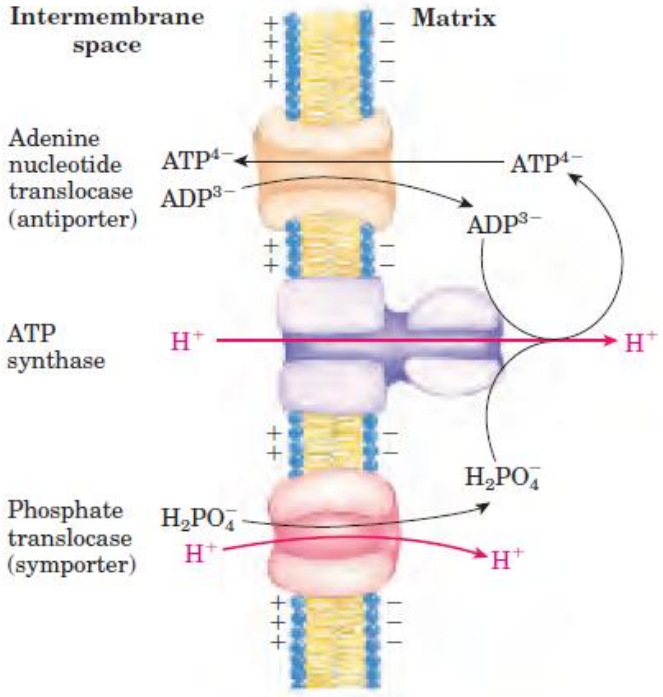


**FIGURE 19–26 Adenine nucleotide and phosphate translocases.** Transport systems of the inner mitochondrial membrane carry ADP and $P_i$ into the matrix and newly synthesized ATP into the cytosol. The adenine nucleotide translocase is an antiporter; the same protein moves ADP into the matrix and ATP out. The effect of replacing $ATP^{4-}$ with $ADP^{3-}$ is the net efflux of one negative charge, which is favored by the charge difference across the inner membrane (outside positive). At pH 7, $P_i$ is present as both $HPO_4^{2-}$ and $H_2PO_4^-$; the phosphate translocase is specific for $H_2PO_4^-$. There is no net flow of charge during symport of $H_2PO_4^-$ and $H^+$, but the relatively low proton concentration in the matrix favors the inward movement of $H^+$. Thus the proton-motive force is responsible both for providing the energy for ATP synthesis and for transporting substrates (ADP and $P_i$) in and product (ATP) out of the mitochondrial matrix. All three of these transport systems can be isolated as a single membrane-bound complex (ATP synthasome).

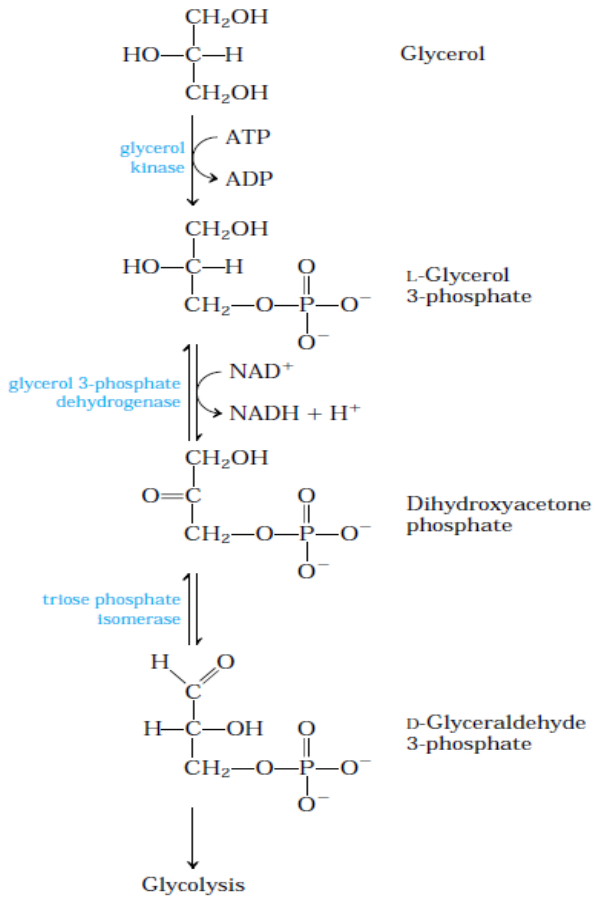


**FIGURE 17–4** Entry of glycerol into the glycolytic pathway.

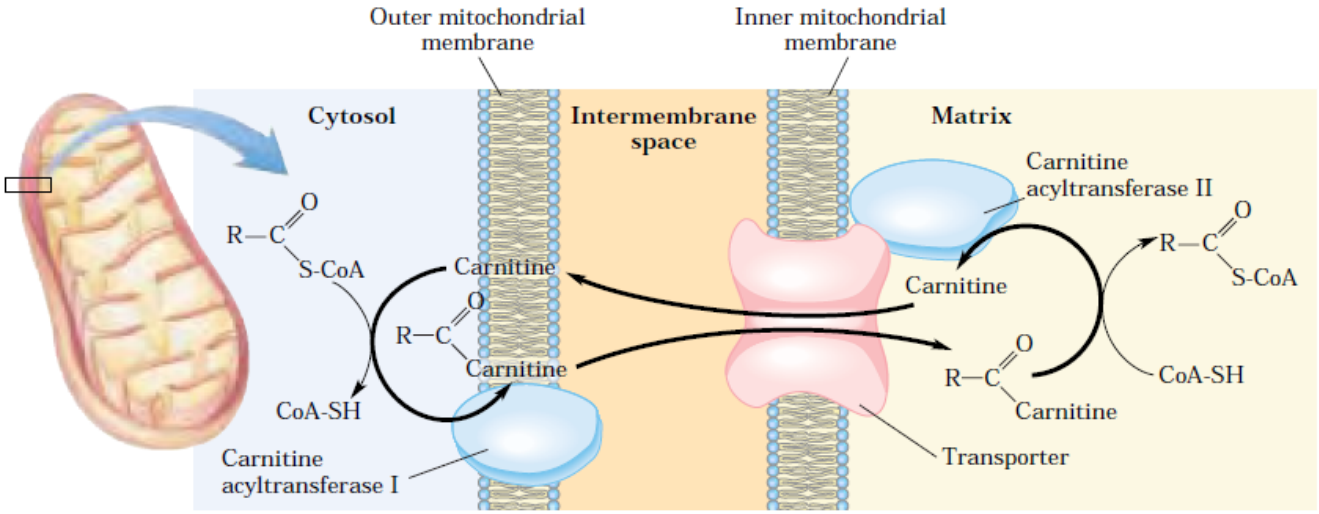


**FIGURE 17–6** **Fatty acid entry into mitochondria via the acyl-carnitine/carnitine transporter.** After fatty acyl–carnitine is formed at the outer membrane or in the intermembrane space, it moves into the matrix by facilitated diffusion through the transporter in the inner membrane. In the matrix, the acyl group is transferred to mitochondrial coenzyme A, freeing carnitine to return to the intermembrane space through the same transporter. Acyltransferase I is inhibited by malonyl-CoA, the first intermediate in fatty acid synthesis (see Fig. 21–1). This inhibition prevents the simultaneous synthesis and degradation of fatty acids.

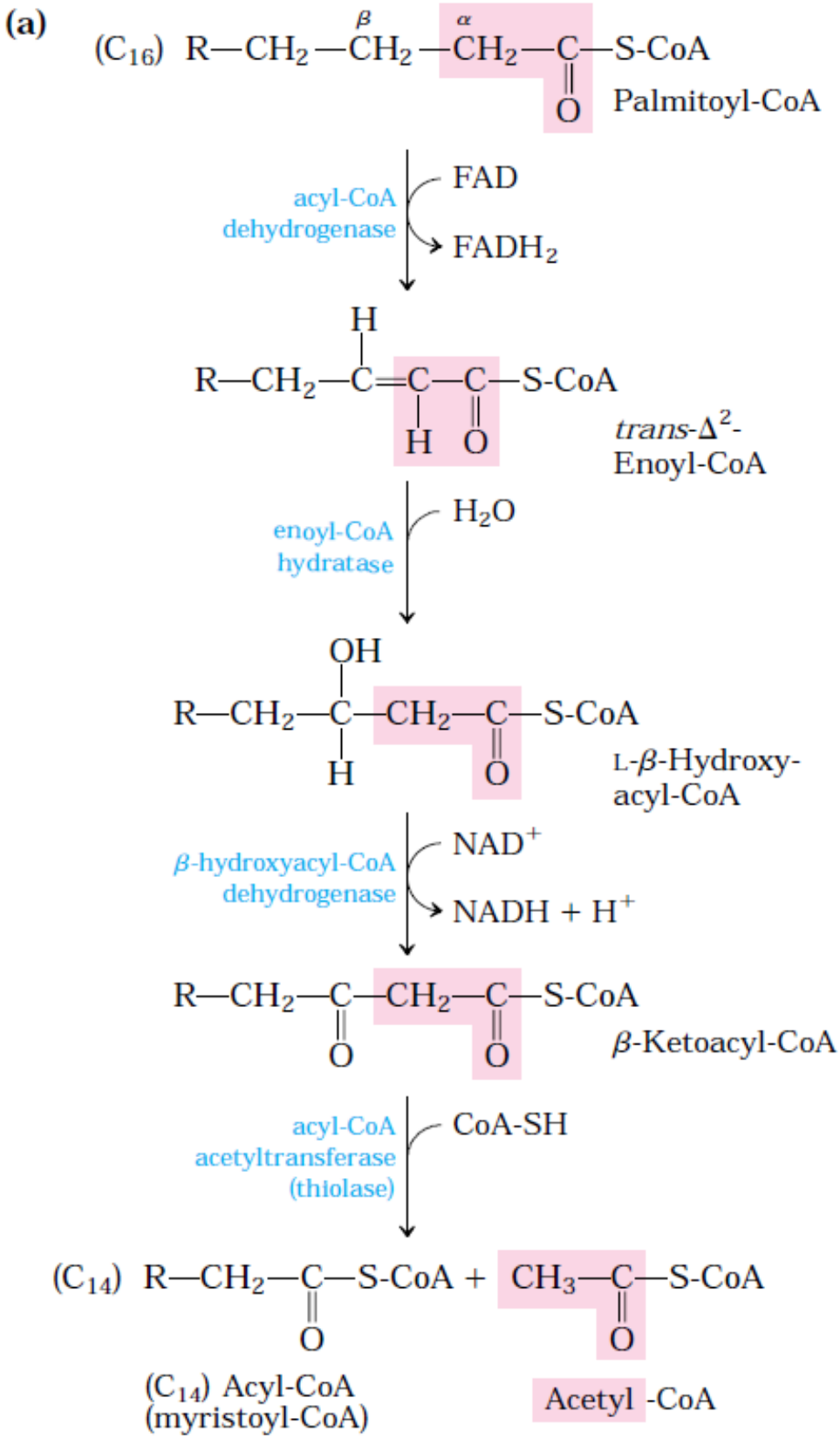
(a)
(C16) R—CH2—CH2—CH2—C—S-CoA
β
α
O
Palmitoyl-CoA
acyl-CoA dehydrogenase
FAD
FADH2
H
R—CH2—C=C—C—S-CoA
H O
trans-Δ2-Enoyl-CoA
enoyl-CoA hydratase
H2O
OH
R—CH2—C—CH2—C—S-CoA
H O
L-β-Hydroxy-acyl-CoA
β-hydroxyacyl-CoA dehydrogenase
NAD+
NADH + H+
R—CH2—C—CH2—C—S-CoA
O O
β-Ketoacyl-CoA
acyl-CoA acetyltransferase (thiolase)
CoA-SH
(C14) R—CH2—C—S-CoA + CH3—C—S-CoA
O O
(C14) Acyl-CoA (myristoyl-CoA)
Acetyl -CoA

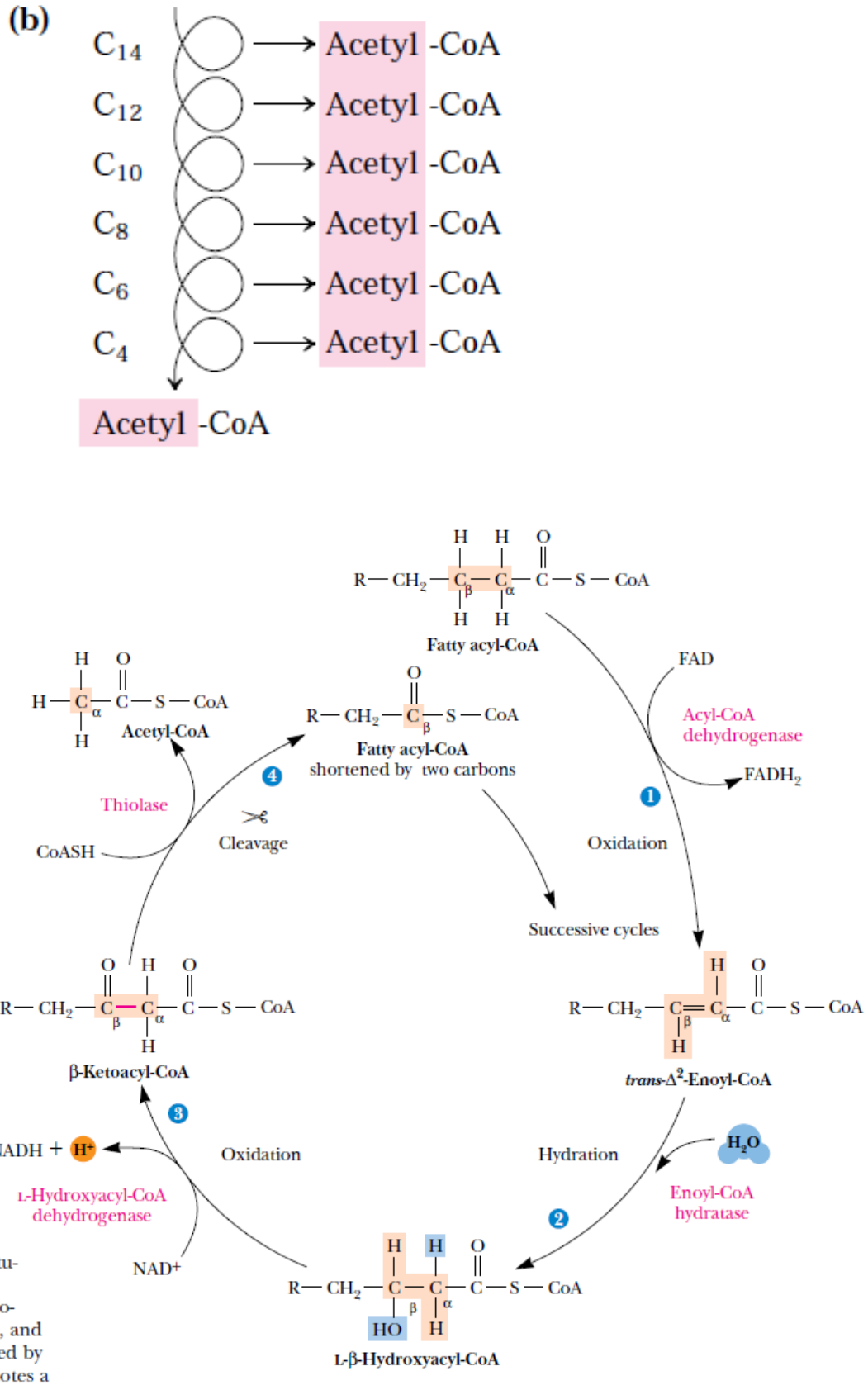


**FIGURE 24.10** • The $\beta$-oxidation of saturated fatty acids involves a cycle of four enzyme-catalyzed reactions. Each cycle produces single molecules of $FADH_2$, NADH, and acetyl-CoA and yields a fatty acid shortened by two carbons. (The delta [Δ] symbol connotes a double bond, and its superscript indicates the lower-numbered carbon involved.)

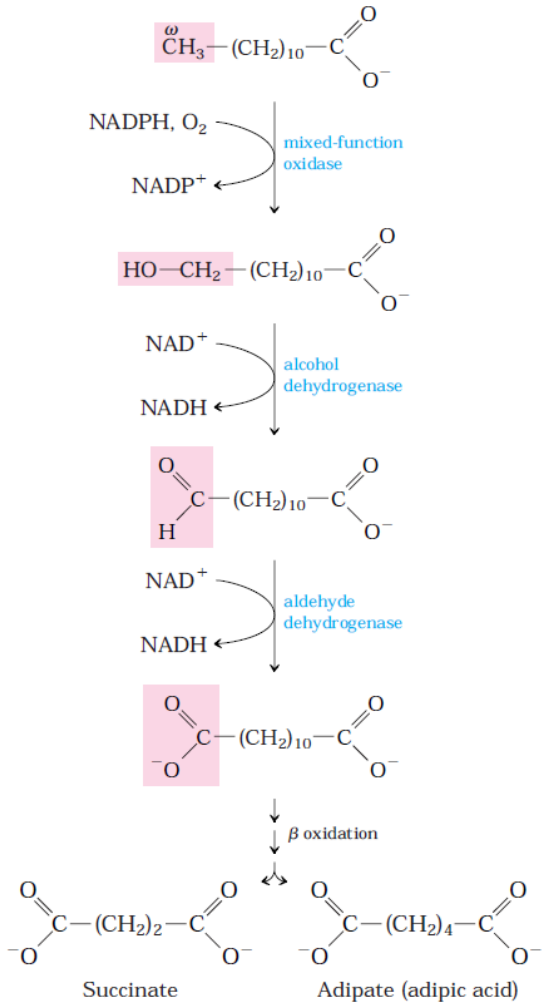


**FIGURE 17–16 The ω oxidation of fatty acids in the endoplasmic reticulum.** This alternative to β oxidation begins with oxidation of the carbon most distant from the α carbon—the ω (omega) carbon. The substrate is usually a medium-chain fatty acid; shown here is lauric acid (laurate). This pathway is generally not the major route for oxidative catabolism of fatty acids.

ter the mitochondrion and undergo β oxidation by the normal route. In each pass through the β-oxidation pathway, the "double-ended" fatty acid yields dicarboxylic acids such as succinic acid, which can enter the citric acid cycle, and adipic acid (Fig. 17–16).

## Phytanic Acid Undergoes α Oxidation in Peroxisomes

The presence of a methyl group on the β carbon of a fatty acid makes β oxidation impossible, and these branched fatty acids are catabolized in peroxisomes of animal cells by **α oxidation.** In the oxidation of phytanic acid, for example (Fig. 17–17), phytanoyl-CoA is hydroxylated on its α carbon, in a reaction that involves molecular oxygen; decarboxylated to form an aldehyde one carbon shorter; and then oxidized to the

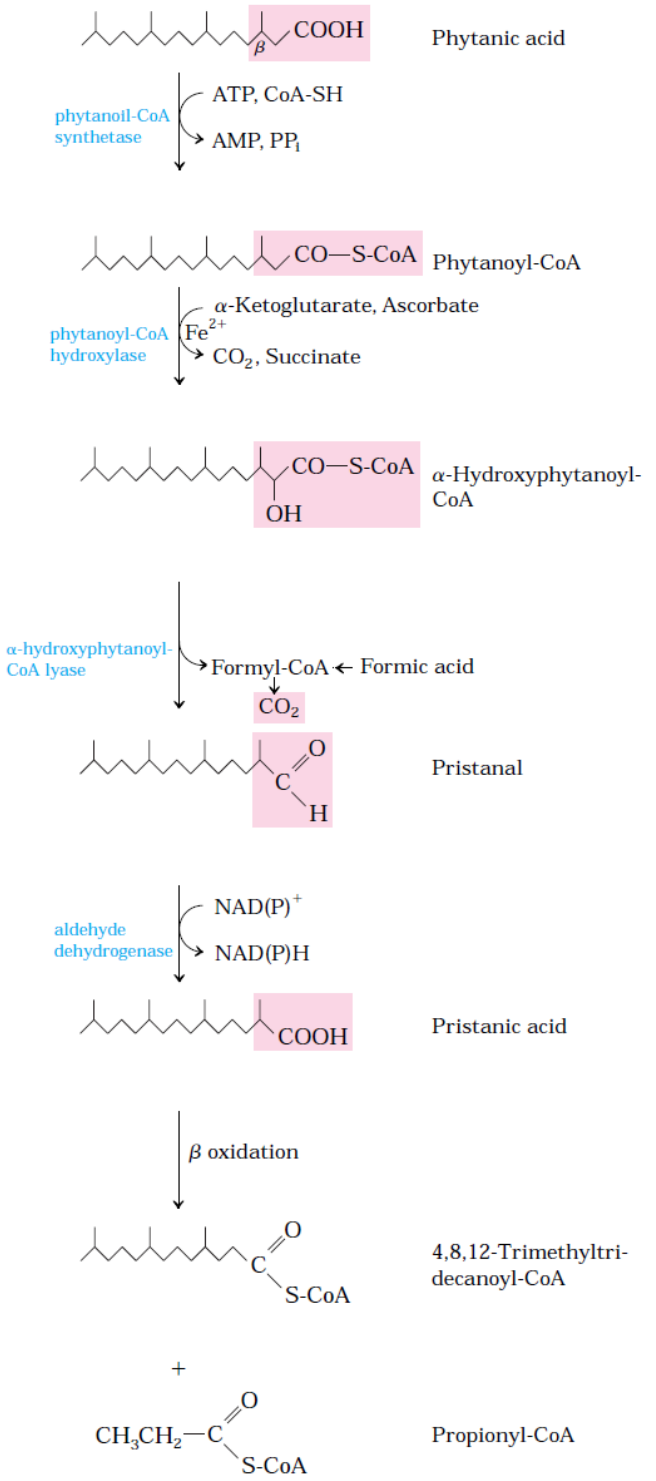


**FIGURE 17–17 The α oxidation of a branched-chain fatty acid (phytanic acid) in peroxisomes.** Phytanic acid has a methyl-substituted β carbon and therefore cannot undergo β oxidation. The combined action of the enzymes shown here removes the carboxyl carbon of phytanic acid, to produce pristanic acid, in which the β carbon is unsubstituted, allowing oxidation. Notice that β oxidation of pristanic acid releases propionyl-CoA, not acetyl-CoA. This is further catabolized as in Figure 17–11. (The details of the reaction that produces pristanal remain controversial.)

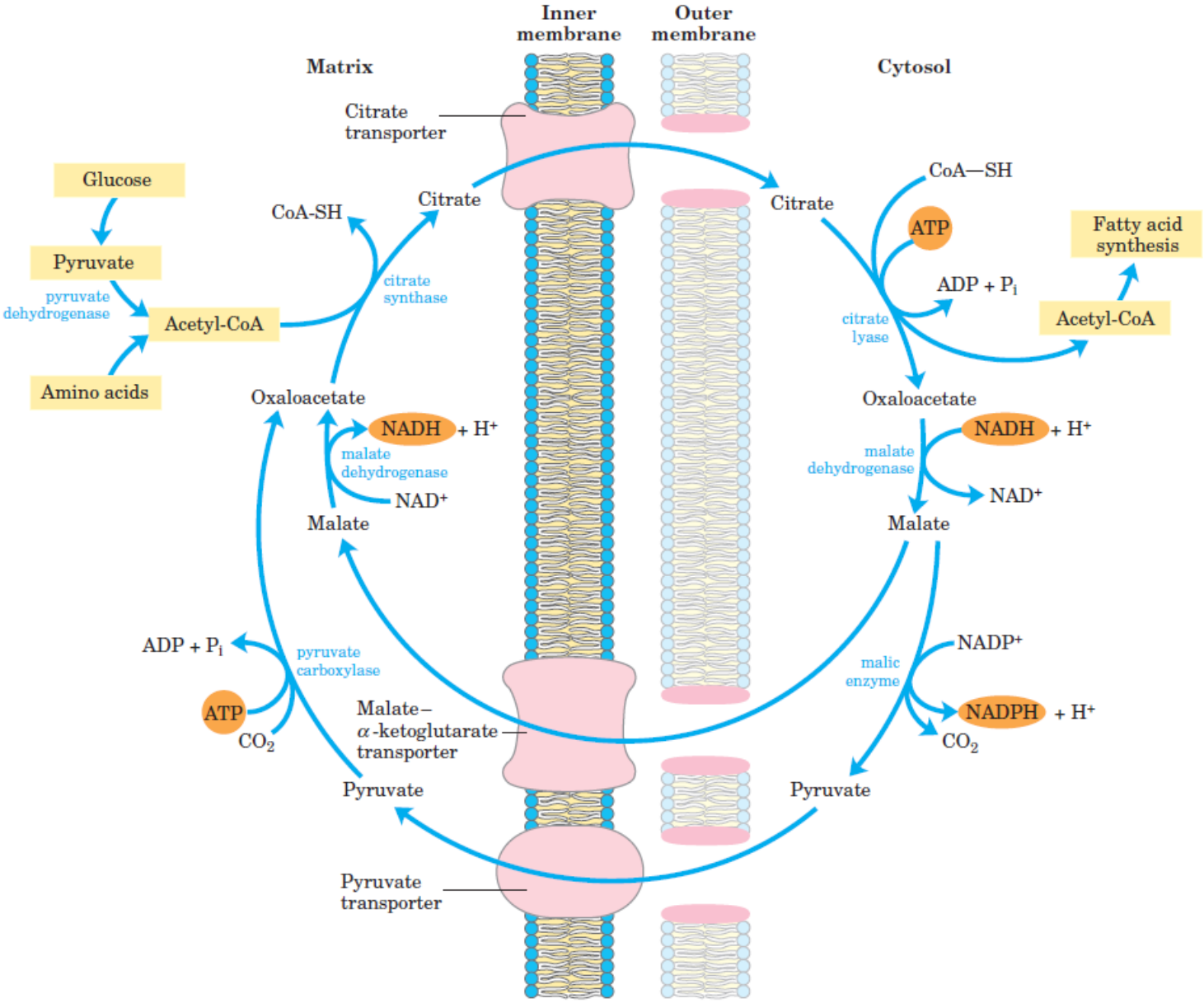


**FIGURE 21–10 Shuttle for transfer of acetyl groups from mitochondria to the cytosol.** The mitochondrial outer membrane is freely permeable to all these compounds. Pyruvate derived from amino acid catabolism in the mitochondrial matrix, or from glucose by glycolysis in the cytosol, is converted to acetyl-CoA in the matrix. Acetyl groups pass out of the mitochondrion as citrate; in the cytosol they are delivered as acetyl-CoA for fatty acid synthesis. Oxaloacetate is reduced to malate, which returns to the mitochondrial matrix and is converted to oxaloacetate. An alternative fate for cytosolic malate is oxidation by malic enzyme to generate cytosolic NADPH; the pyruvate produced returns to the mitochondrial matrix.

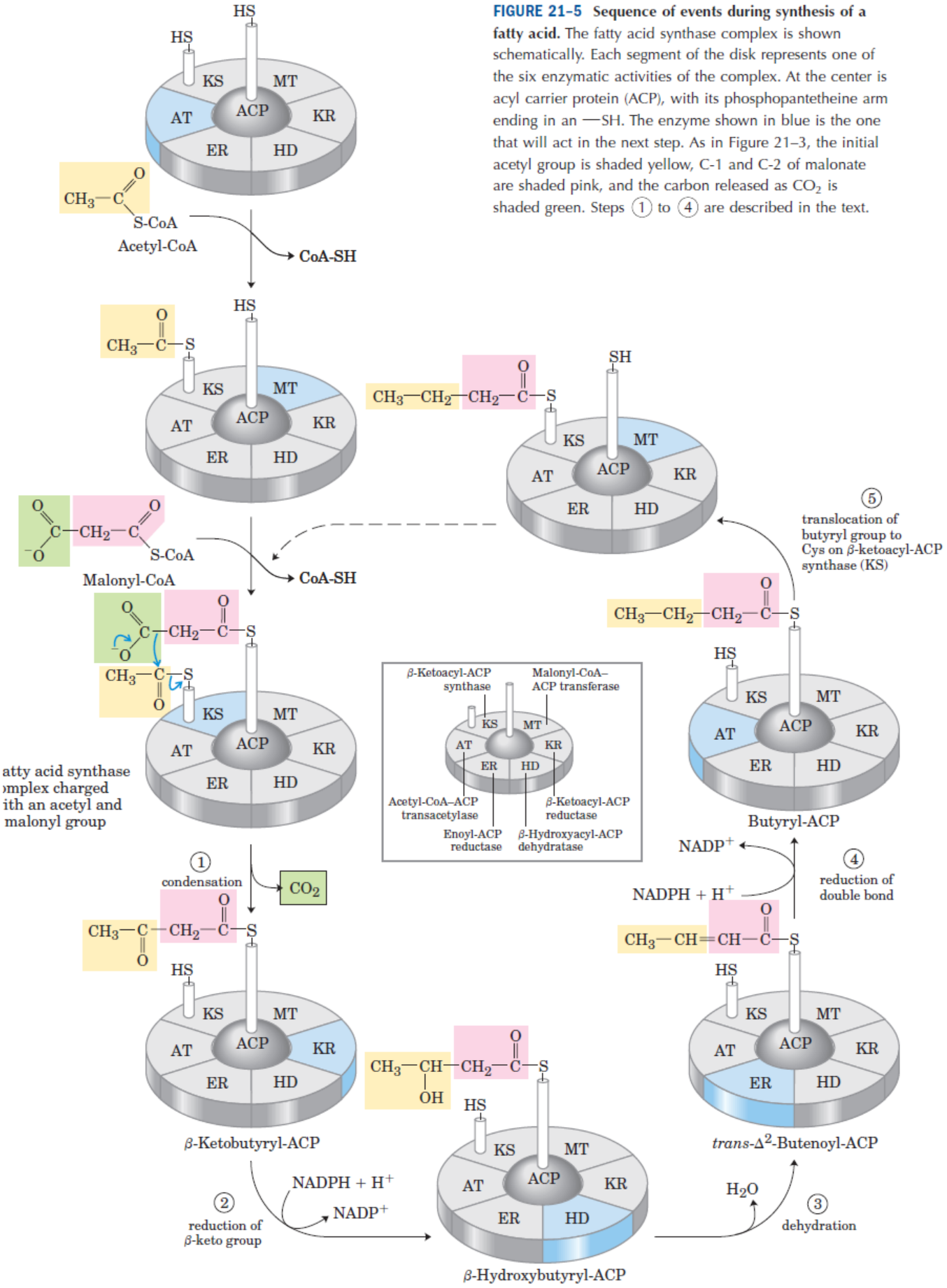


**FIGURE 21–5 Sequence of events during synthesis of a fatty acid.** The fatty acid synthase complex is shown schematically. Each segment of the disk represents one of the six enzymatic activities of the complex. At the center is acyl carrier protein (ACP), with its phosphopantetheine arm ending in an —SH. The enzyme shown in blue is the one that will act in the next step. As in Figure 21–3, the initial acetyl group is shaded yellow, C-1 and C-2 of malonate are shaded pink, and the carbon released as $CO_2$ is shaded green. Steps (1) to (4) are described in the text.

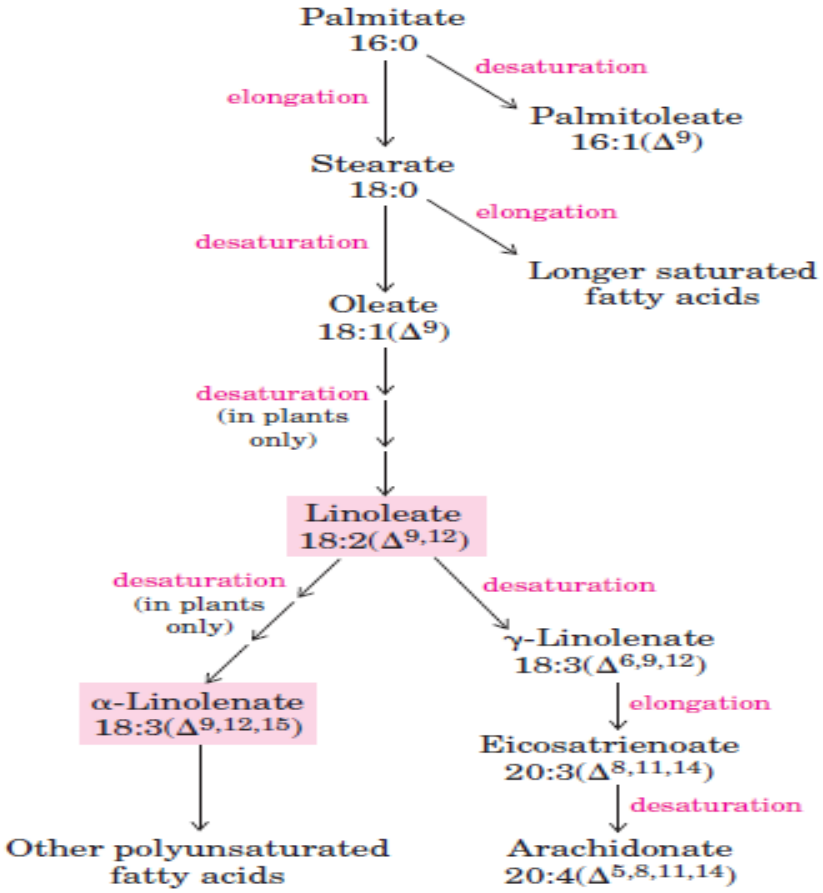


**FIGURE 21–12 Routes of synthesis of other fatty acids.** Palmitate is the precursor of stearate and longer-chain saturated fatty acids, as well as the monounsaturated acids palmitoleate and oleate. Mammals cannot convert oleate to linoleate or α-linolenate (shaded pink), which are therefore required in the diet as essential fatty acids. Conversion of linoleate to other polyunsaturated fatty acids and eicosanoids is outlined. Unsaturated fatty acids are symbolized by indicating the number of carbons and the number and position of the double bonds, as in Table 10–1.

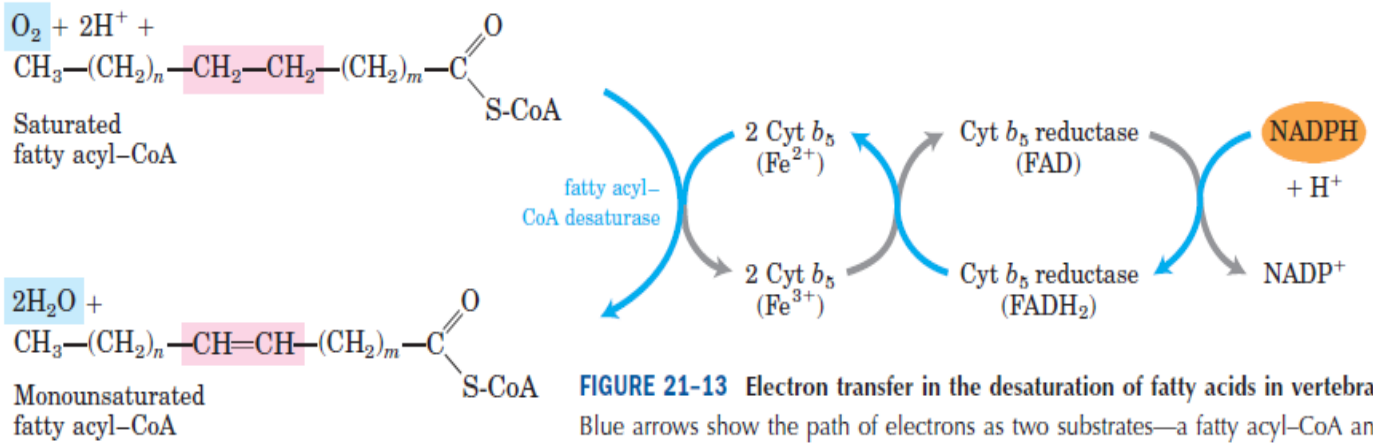


**FIGURE 21-13 Electron transfer in the desaturation of fatty acids in vertebrates.** Blue arrows show the path of electrons as two substrates—a fatty acyl–CoA and NADPH—undergo oxidation by molecular oxygen. These reactions take place on the lumenal face of the smooth ER. A similar pathway, but with different electron carriers, occurs in plants.

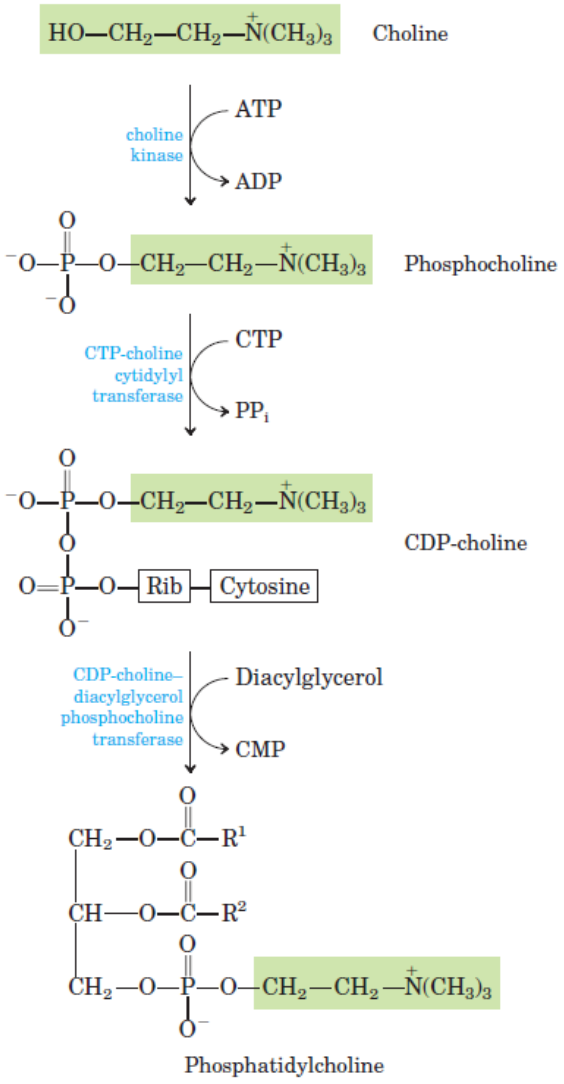


**FIGURE 21–28 Pathway for phosphatidylcholine synthesis from choline in mammals.** The same strategy shown here (strategy 2 in Fig. 21–24) is also used for salvaging ethanolamine in phosphatidylethanolamine synthesis.

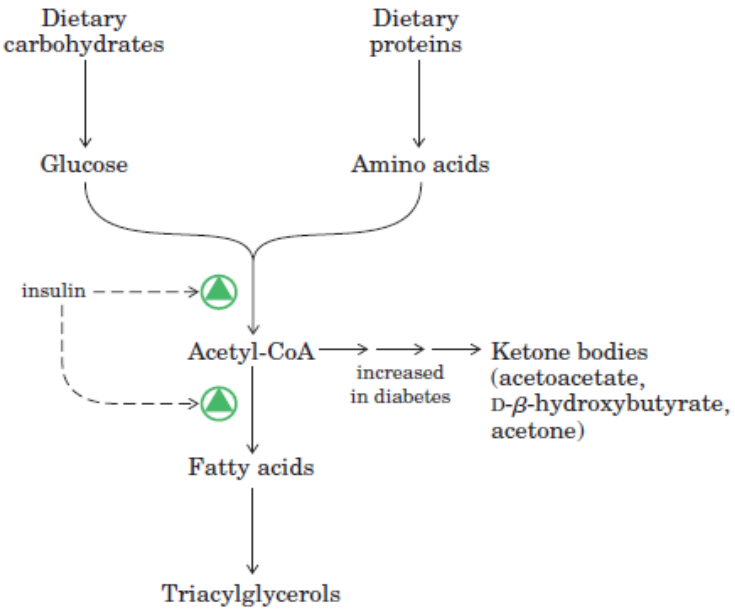


**FIGURE 21–19 Regulation of triacylglycerol synthesis by insulin.** Insulin stimulates conversion of dietary carbohydrates and proteins to fat. Individuals with diabetes mellitus lack insulin; in uncontrolled disease, this results in diminished fatty acid synthesis, and the acetyl-CoA arising from catabolism of carbohydrates and proteins is shunted instead to ketone body production. People in severe ketosis smell of acetone, so the condition is sometimes mistaken for drunkenness (p. 909).

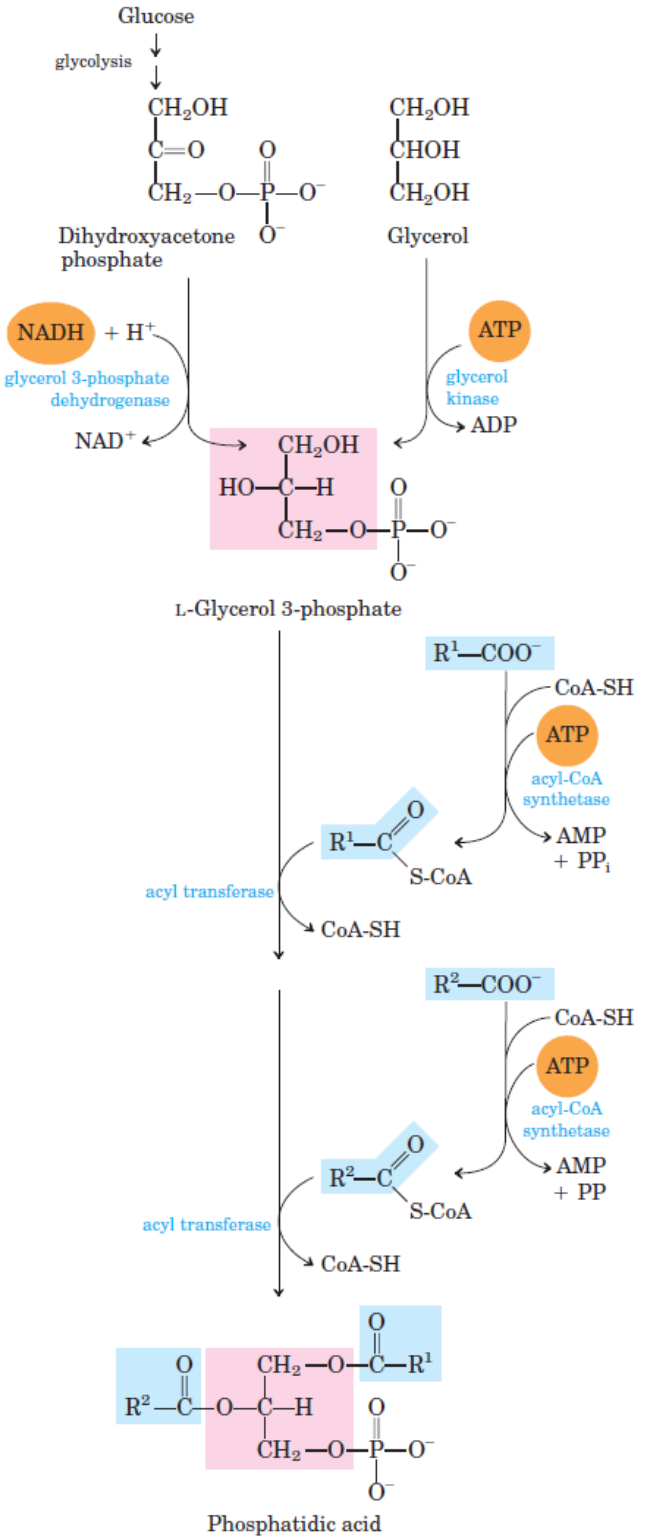


**FIGURE 21–17 Biosynthesis of phosphatidic acid.** A fatty acyl group is activated by formation of the fatty acyl–CoA, then transferred to ester linkage with L-glycerol 3-phosphate, formed in either of the two ways shown. Phosphatidic acid is shown here with the correct stereochemistry at C-2 of the glycerol molecule. To conserve space in subsequent figures (and in Fig. 21–14), both fatty acyl groups of glycerophospholipids, and all three acyl groups of triacylglycerols, are shown projecting to the right.

carbohydrates or amino acids. If the diabetes is untreated, these individuals have increased rates of fat oxidation and ketone body formation (Chapter 17) and therefore lose weight. ■

An additional factor in the balance between biosynthesis and degradation of triacylglycerols is that approximately 75% of all fatty acids released by lipolysis are reesterified to form triacylglycerols rather than used for fuel. This ratio persists even under starvation conditions, when energy metabolism is shunted from the use of carbohydrate to the oxidation of fatty acids. Some of this fatty acid recycling takes place in adipose tissue, with the reesterification occurring before release into the bloodstream; some takes place via a systemic cycle in which free fatty acids are transported to liver, recycled to triacylglycerol, exported again to the blood (transport of lipids in the blood is discussed in Section 21.4), and taken up again by adipose tissue after release from triacylglycerol by extracellular lipoprotein lipase

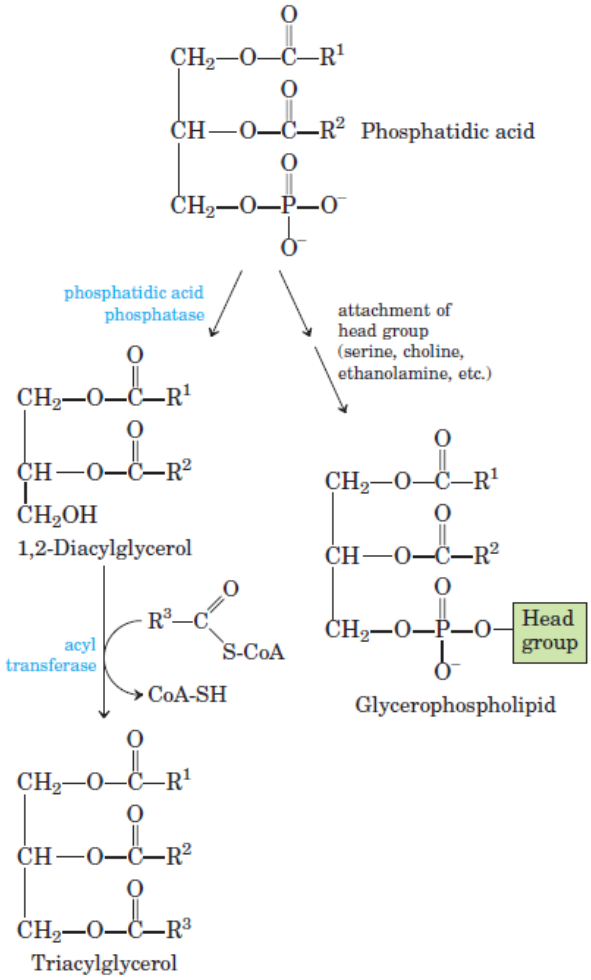


**FIGURE 21–18 Phosphatidic acid in lipid biosynthesis.** Phosphatidic acid is the precursor of both triacylglycerols and glycerophospholipids. The mechanisms for head-group attachment in phospholipid synthesis are described later in this section.

Eugene P. Kennedy

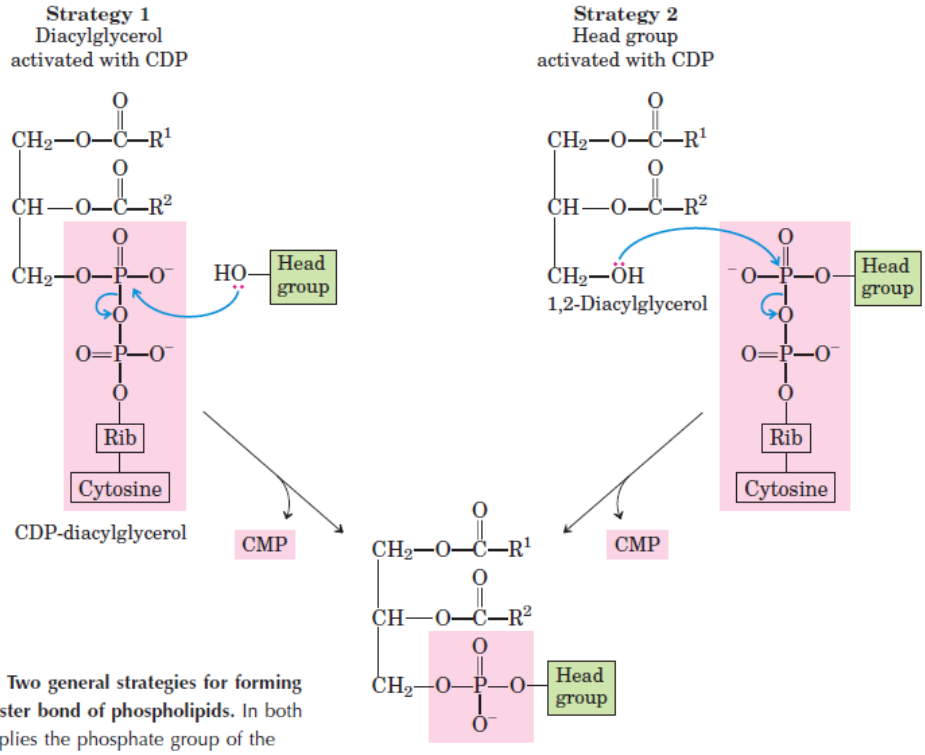


**FIGURE 21-24** **Two general strategies for forming the phosphodiester bond of phospholipids.** In both cases, CDP supplies the phosphate group of the phosphodiester bond.

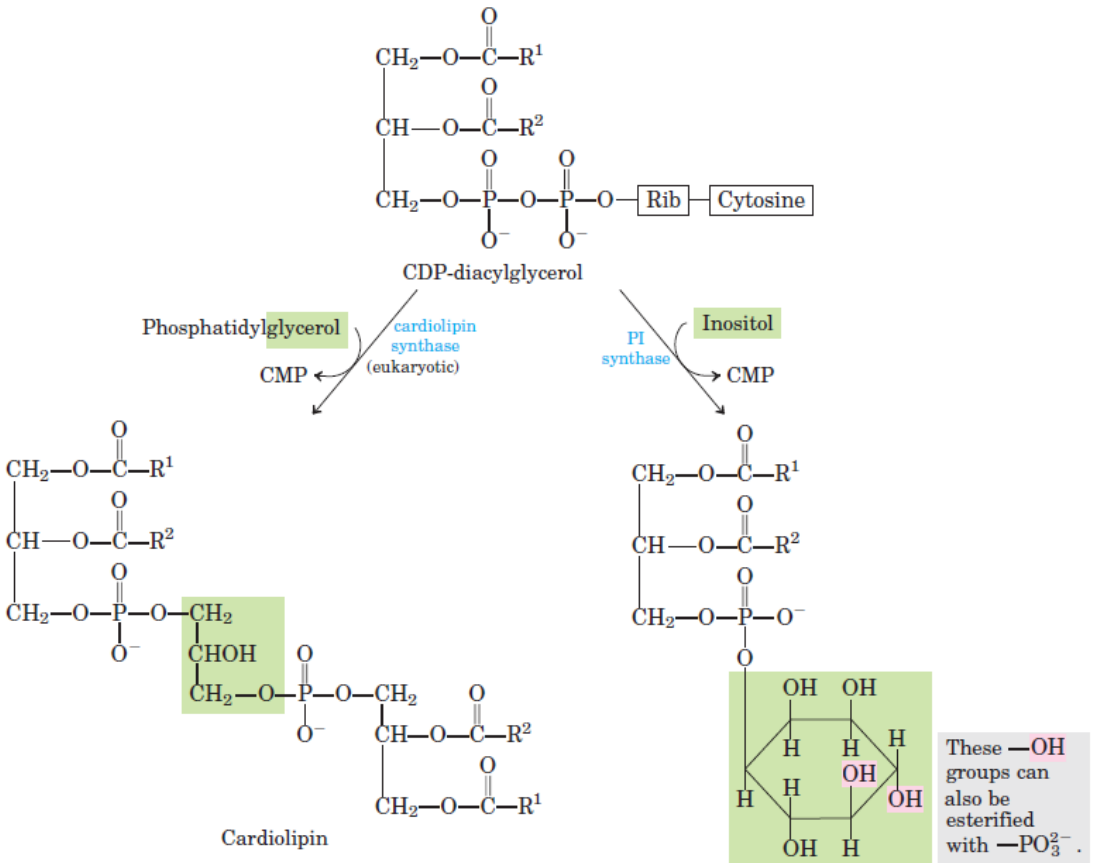


**FIGURE 21-26** **Synthesis of cardiolipin and phosphatidylinositol in eukaryotes.** These glycerophospholipids are synthesized using strategy 1 in Figure 21-24. Phosphatidylglycerol is synthesized as in bacteria (see Fig. 21–25). PI represents phosphatidylinositol.

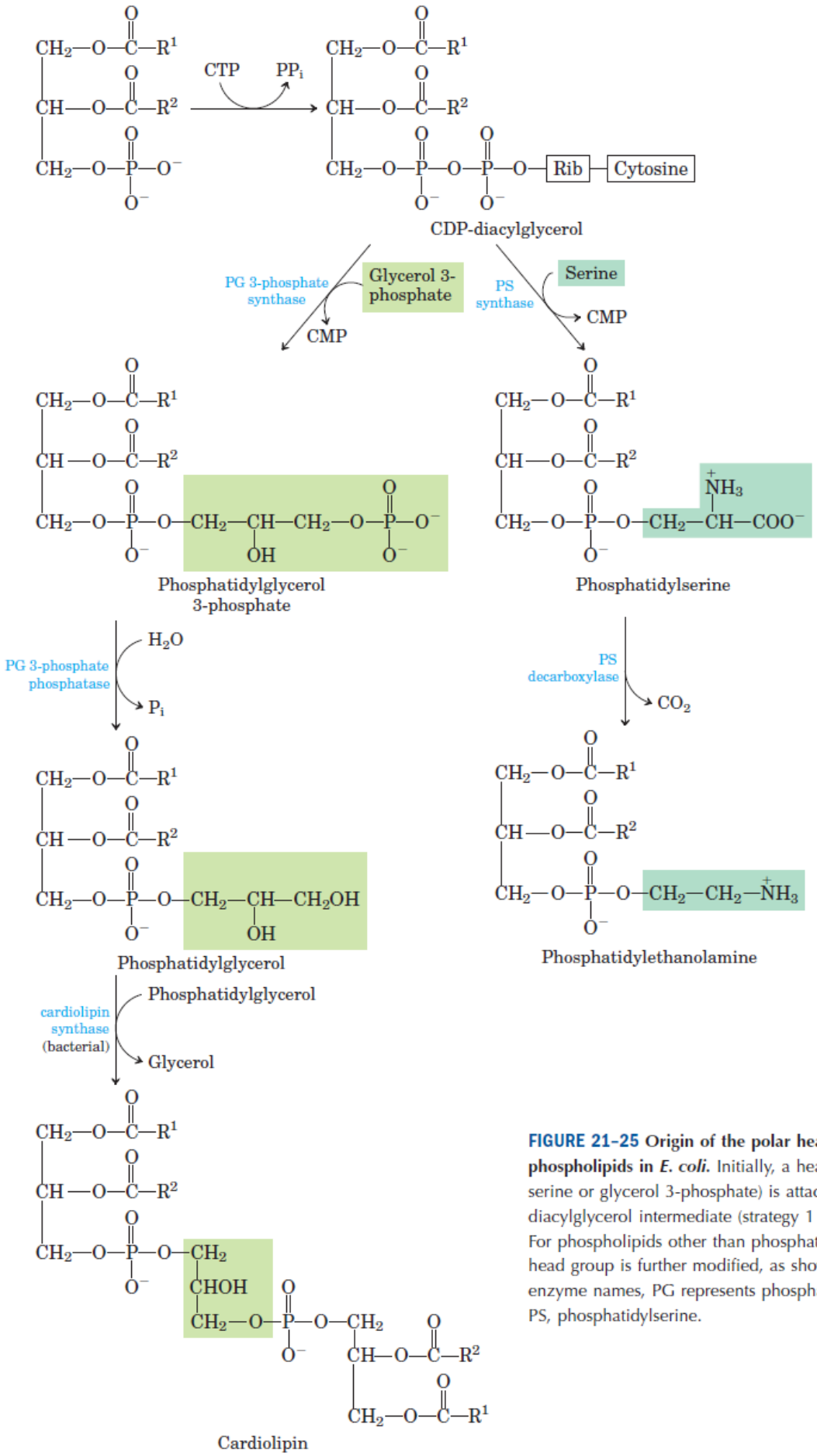


**FIGURE 21–25 Origin of the polar head groups of phospholipids in *E. coli*.** Initially, a head group (either serine or glycerol 3-phosphate) is attached via a CDP-diacylglycerol intermediate (strategy 1 in Fig. 21–24). For phospholipids other than phosphatidylserine, the head group is further modified, as shown here. In the enzyme names, PG represents phosphatidylglycerol; PS, phosphatidylserine.

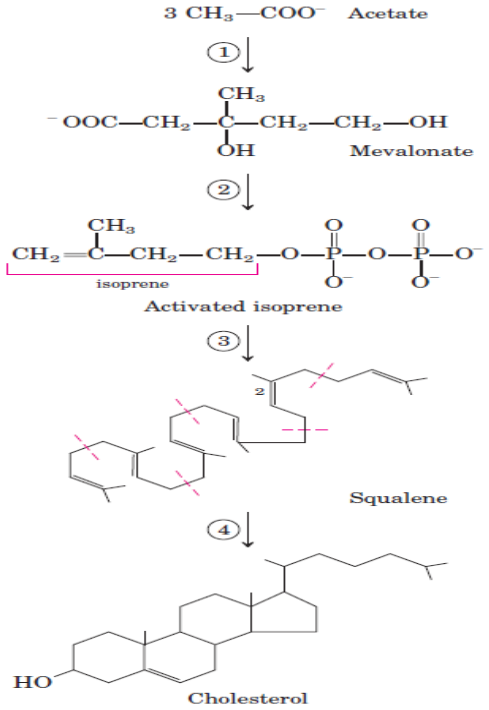


**FIGURE 21–33 Summary of cholesterol biosynthesis.** The four stages are discussed in the text. Isoprene units in squalene are set off by red dashed lines.

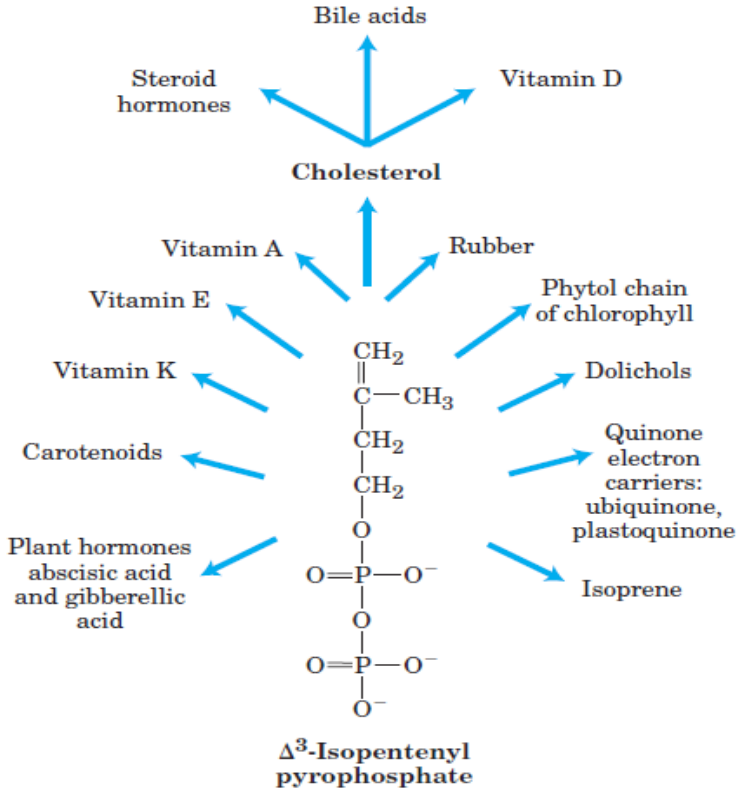


**FIGURE 21–48 Overview of isoprenoid biosynthesis.** The structures of most of the end products shown here are given in Chapter 10.

## TABLE 23–3 Effects of Insulin on Blood Glucose: Uptake of Glucose by Cells and Storage as Triacylglycerols and Glycogen

| *Metabolic effect* | *Target enzyme* |
|---|---|
| ↑ Glucose uptake (muscle, adipose) | ↑ Glucose transporter (GLUT4) |
| ↑ Glucose uptake (liver) | ↑ Glucokinase (increased expression) |
| ↑ Glycogen synthesis (liver, muscle) | ↑ Glycogen synthase |
| ↓ Glycogen breakdown (liver, muscle) | ↓ Glycogen phosphorylase |
| ↑ Glycolysis, acetyl-CoA production (liver, muscle) | ↑ PFK-1 (by ↑ PFK-2)<br>↑ Pyruvate dehydrogenase complex |
| ↑ Fatty acid synthesis (liver) | ↑ Acetyl-CoA carboxylase |
| ↑ Triacylglycerol synthesis (adipose tissue) | ↑ Lipoprotein lipase |

## TABLE 23–6 Physiological and Metabolic Effects of Epinephrine: Preparation for Action

| *Immediate effect* | *Overall effect* |
|---|---|
| **Physiological** | |
| ↑ Heart rate<br>↑ Blood pressure<br>↑ Dilation of respiratory passages | Increase delivery of $O_2$ to tissues (muscle) |
| **Metabolic** | |
| ↑ Glycogen breakdown (muscle, liver)<br>↓ Glycogen synthesis (muscle, liver)<br>↑ Gluconeogenesis (liver) | Increase production of glucose for fuel |
| ↑ Glycolysis (muscle) | Increases ATP production in muscle |
| ↑ Fatty acid mobilization (adipose tissue) | Increases availability of fatty acids as fuel |
| ↑ Glucagon secretion<br>↓ Insulin secretion | Reinforce metabolic effects of epinephrine |

## TABLE 23–4 Effects of Glucagon on Blood Glucose: Production and Release of Glucose by the Liver

| *Metabolic effect* | *Effect on glucose metabolism* | *Target enzyme* |
|---|---|---|
| ↑ Glycogen breakdown (liver) | Glycogen ⟶ glucose | ↑ Glycogen phosphorylase |
| ↓ Glycogen synthesis (liver) | Less glucose stored as glycogen | ↓ Glycogen synthase |
| ↓ Glycolysis (liver) | Less glucose used as fuel in liver | ↓ PFK-1 |
| ↑ Gluconeogenesis (liver) | Amino acids, Glycerol, Oxaloacetate ⟶ glucose | ↑ FBPase-2<br>↓ Pyruvate kinase<br>↑ PEP carboxykinase |
| ↑ Fatty acid mobilization (adipose tissue) | Less glucose used as fuel by liver, muscle | ↑ Triacylglycerol lipase<br>Perilipin phosphorylation |
| ↑ Ketogenesis | Provides alternative to glucose as energy source for brain | ↑ Acetyl-CoA carboxylase |

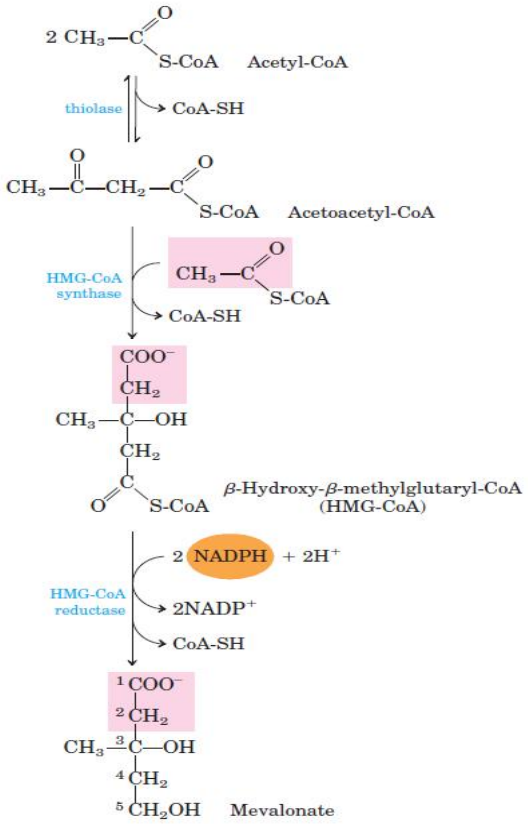


**FIGURE 21–34** **Formation of mevalonate from acetyl-CoA.** The origin of C-1 and C-2 of mevalonate from acetyl-CoA is shown in pink.

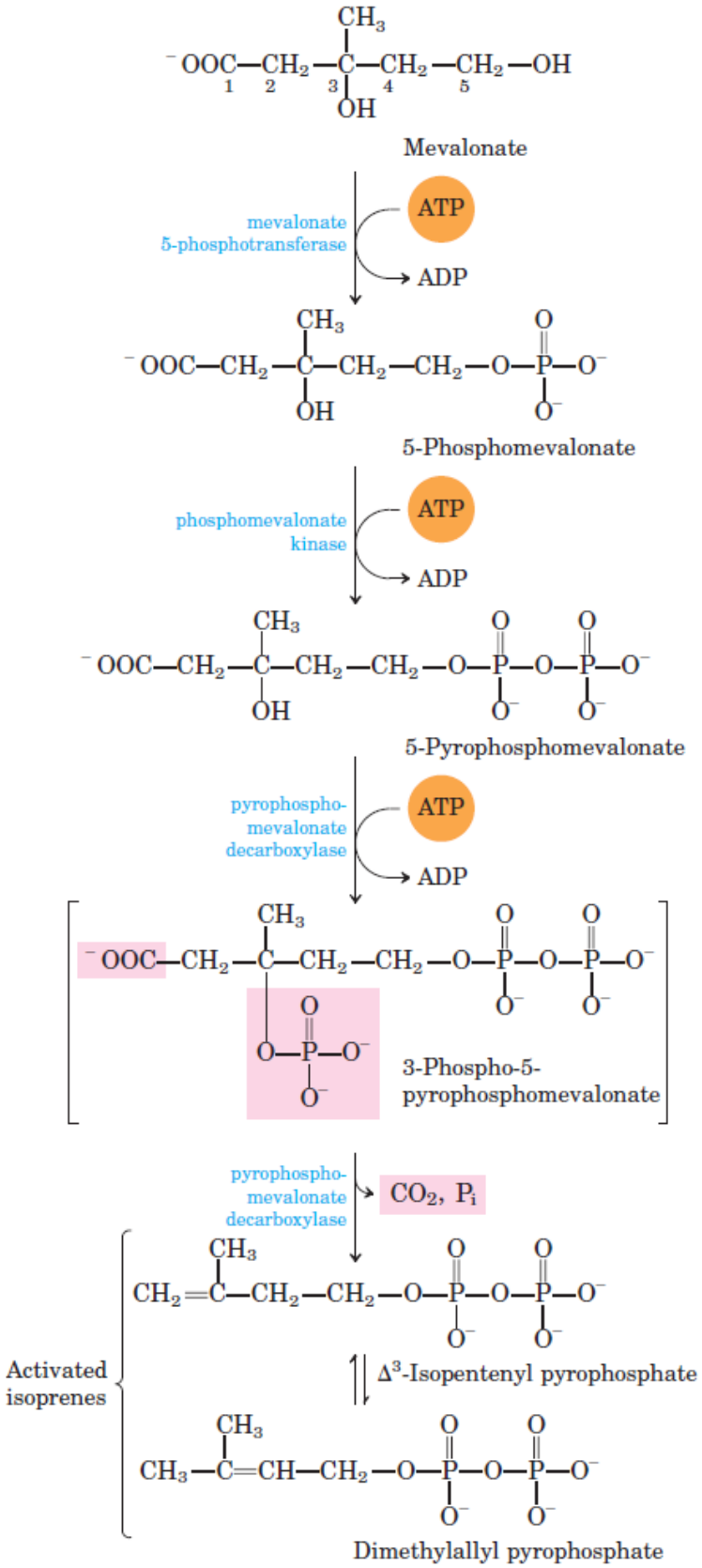


**FIGURE 21–35** **Conversion of mevalonate to activated isoprene units.** Six of these activated units combine to form squalene (see Fig. 21–36). The leaving groups of 3-phospho-5-pyrophosphomevalonate are shaded pink. The bracketed intermediate is hypothetical.

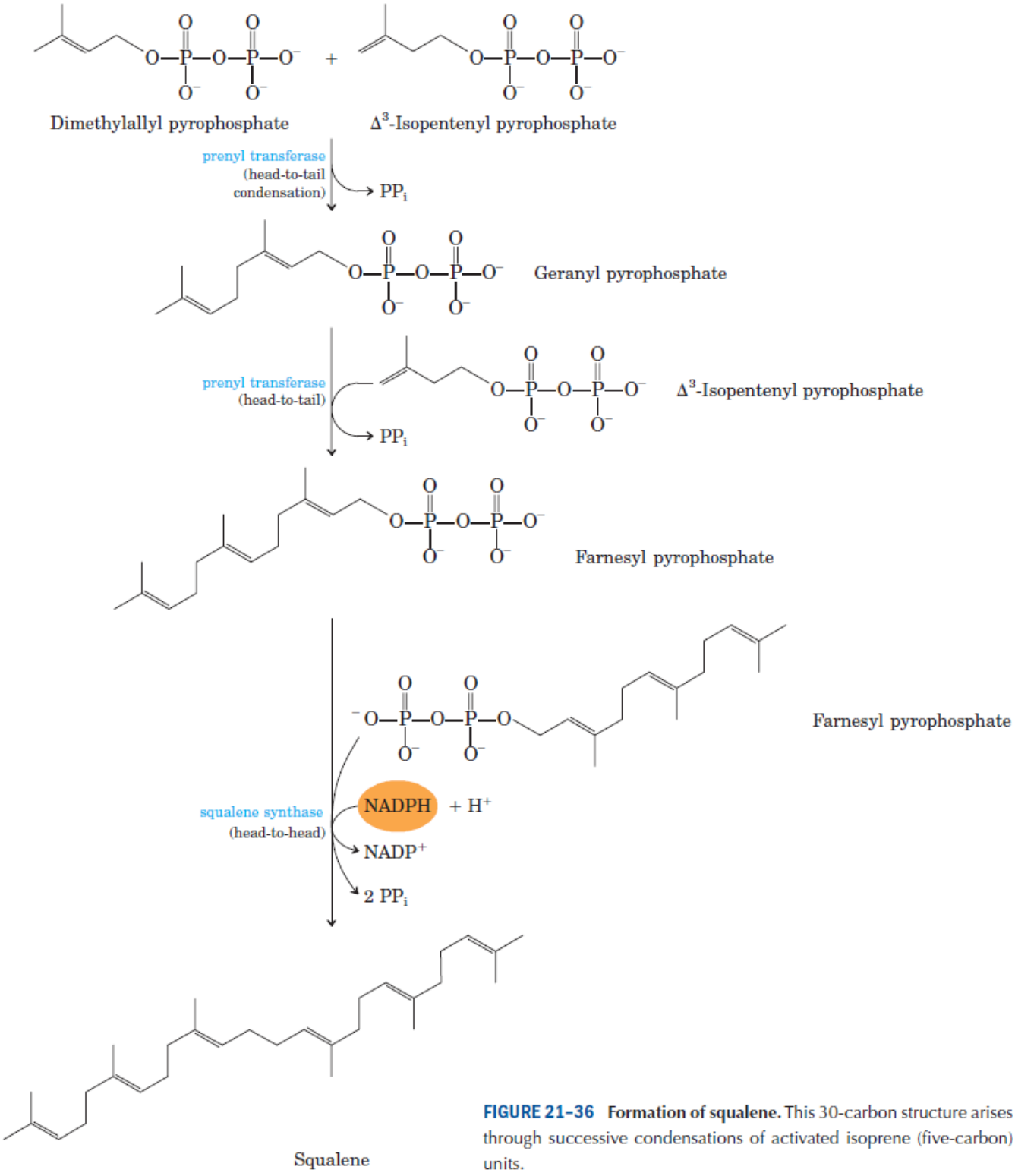


**FIGURE 21–36** **Formation of squalene.** This 30-carbon structure arises through successive condensations of activated isoprene (five-carbon) units.

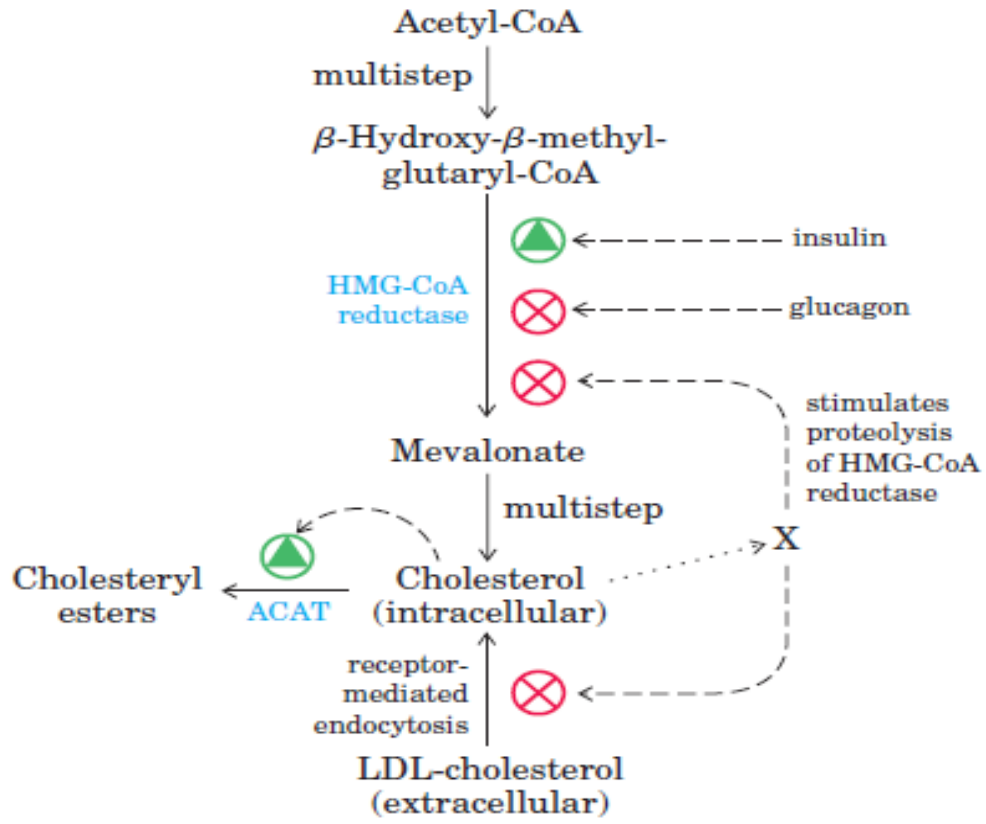


**FIGURE 21-44 Regulation of cholesterol formation balances synthesis with dietary uptake.** Glucagon promotes phosphorylation (inactivation) of HMG-CoA reductase; insulin promotes dephosphorylation (activation). X represents unidentified metabolites of cholesterol that stimulate proteolysis of HMG-CoA reductase.

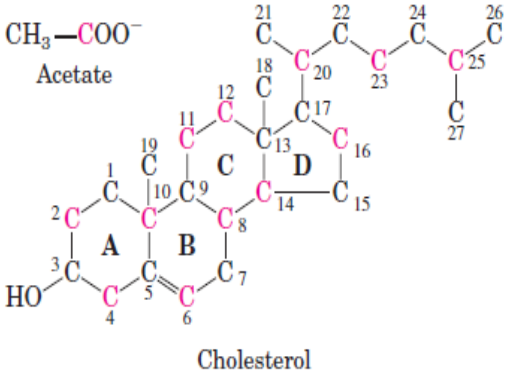


**FIGURE 21-32 Origin of the carbon atoms of cholesterol.** This can be deduced from tracer experiments with acetate labeled in the methyl carbon (black) or the carboxyl carbon (red). The individual rings in the fused-ring system are designated A through D.

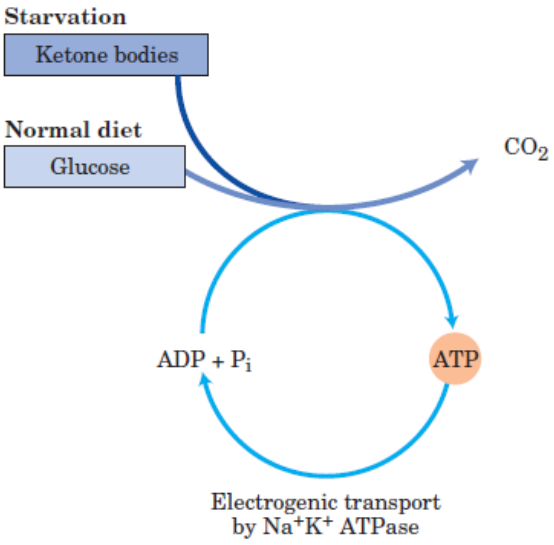


**FIGURE 23-20 Energy sources in the brain vary with nutritional state.** The ketone body used by the brain is β-hydroxybutyrate.

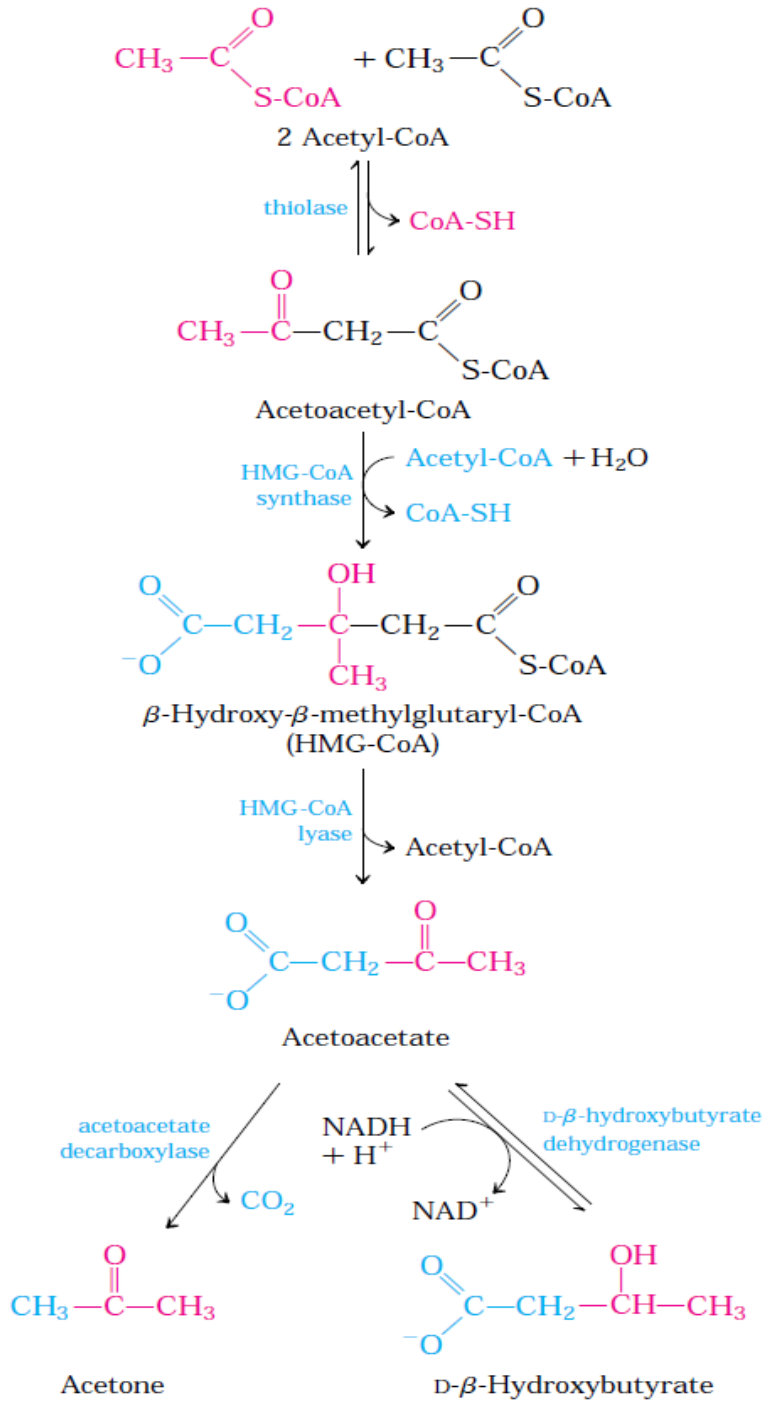


**FIGURE 17–18 Formation of ketone bodies from acetyl-CoA.** Healthy, well-nourished individuals produce ketone bodies at a relatively low rate. When acetyl-CoA accumulates (as in starvation or untreated diabetes, for example), thiolase catalyzes the condensation of two acetyl-CoA molecules to acetoacetyl-CoA, the parent compound of the three ketone bodies. The reactions of ketone body formation occur in the matrix of liver mitochondria. The six-carbon compound β-hydroxy-β-methylglutaryl-CoA (HMG-CoA) is also an intermediate of sterol biosynthesis, but the enzyme that forms HMG-CoA in that pathway is cytosolic. HMG-CoA lyase is present only in the mitochondrial matrix.

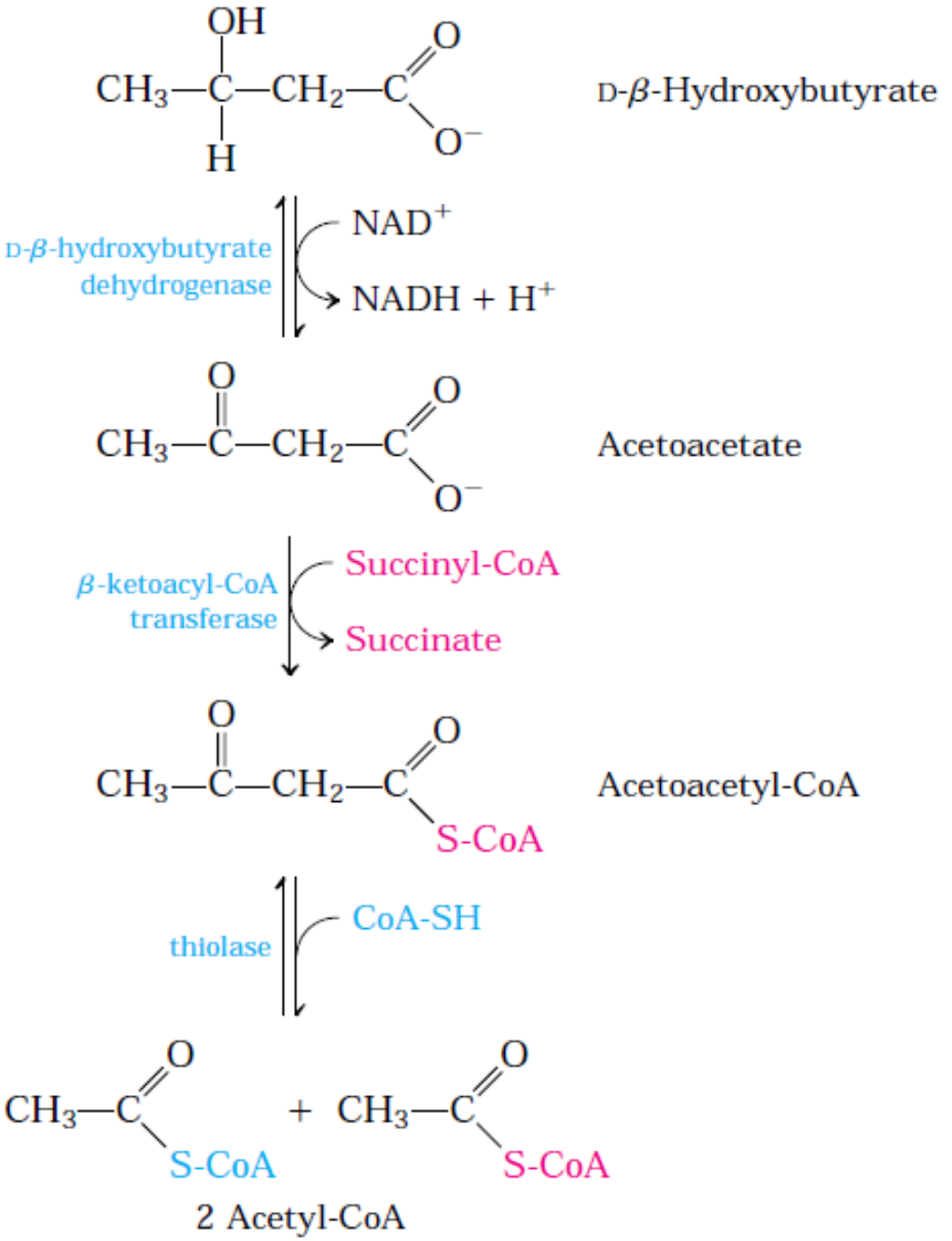


**FIGURE 17–19** **D-β-Hydroxybutyrate as a fuel.** D-β-Hydroxybutyrate, synthesized in the liver, passes into the blood and thus to other tissues, where it is converted in three steps to acetyl-CoA. It is first oxidized to acetoacetate, which is activated with coenzyme A donated from succinyl-CoA, then split by thiolase. The acetyl-CoA thus formed is used for energy production.

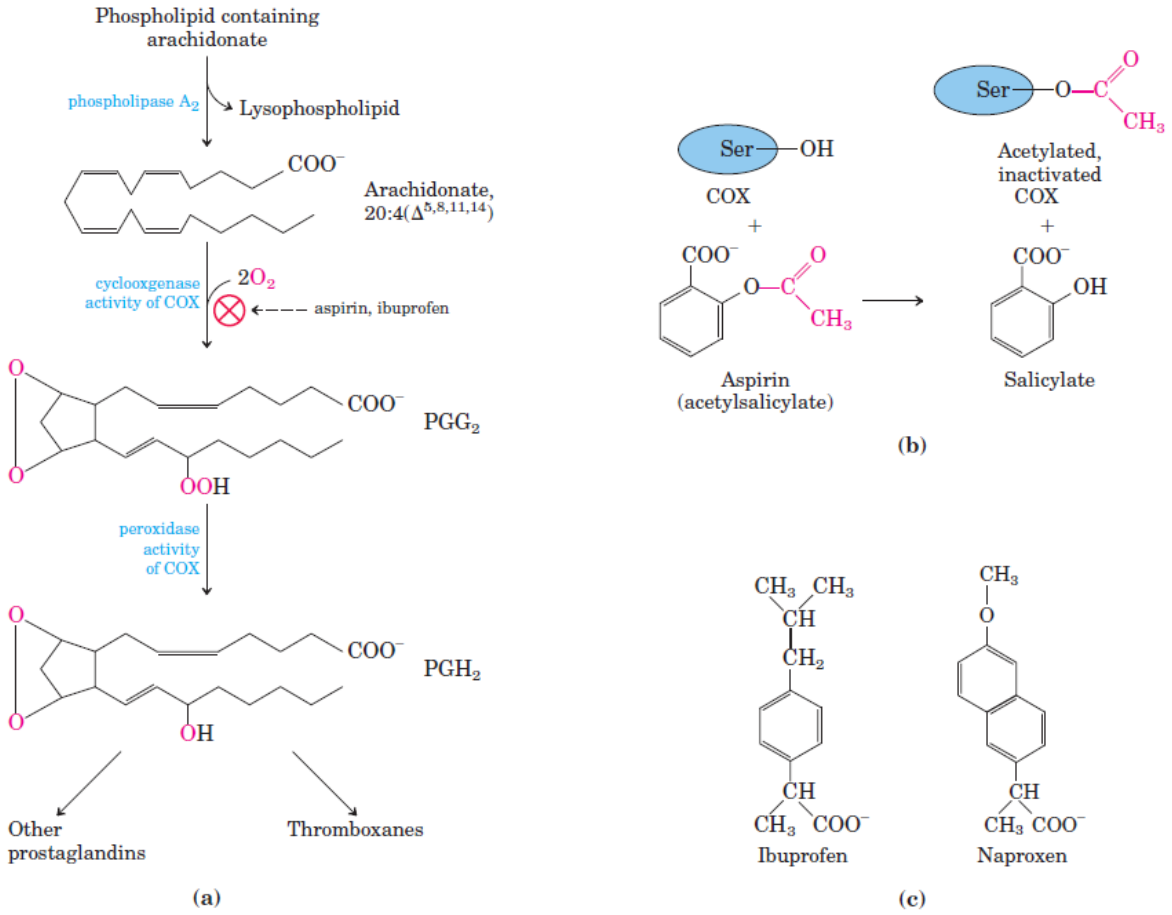


**FIGURE 21–15 The "cyclic" pathway from arachidonate to prostaglandins and thromboxanes.** **(a)** After arachidonate is released from phospholipids by the action of phospholipase $A_2$, the cyclooxygenase and peroxidase activities of COX (also called prostaglandin $H_2$ synthase) catalyze the production of $PGH_2$, the precursor of other prostaglandins and thromboxanes. **(b)** Aspirin inhibits the first reaction by acetylating an essential Ser residue on the enzyme. **(c)** Ibuprofen and naproxen inhibit the same step, probably by mimicking the structure of the substrate or an intermediate in the reaction.

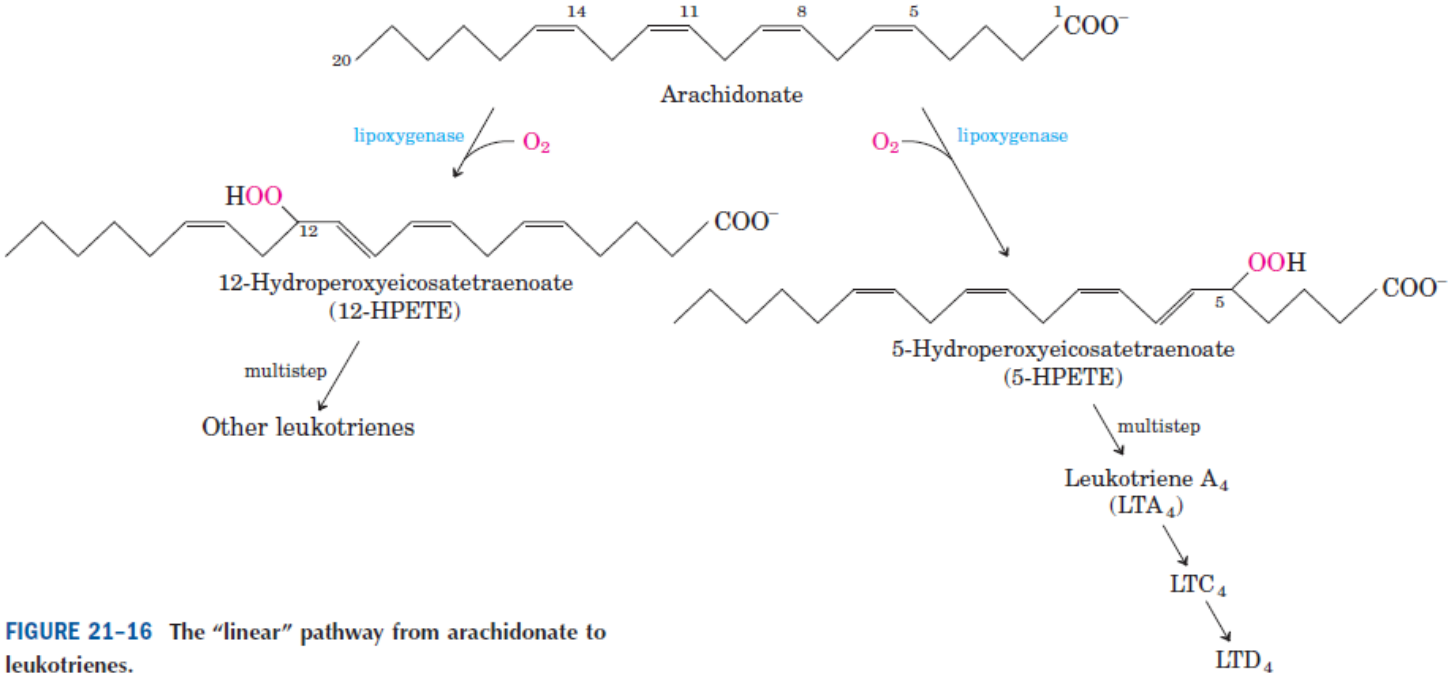


**FIGURE 21–16 The "linear" pathway from arachidonate to leukotrienes.**

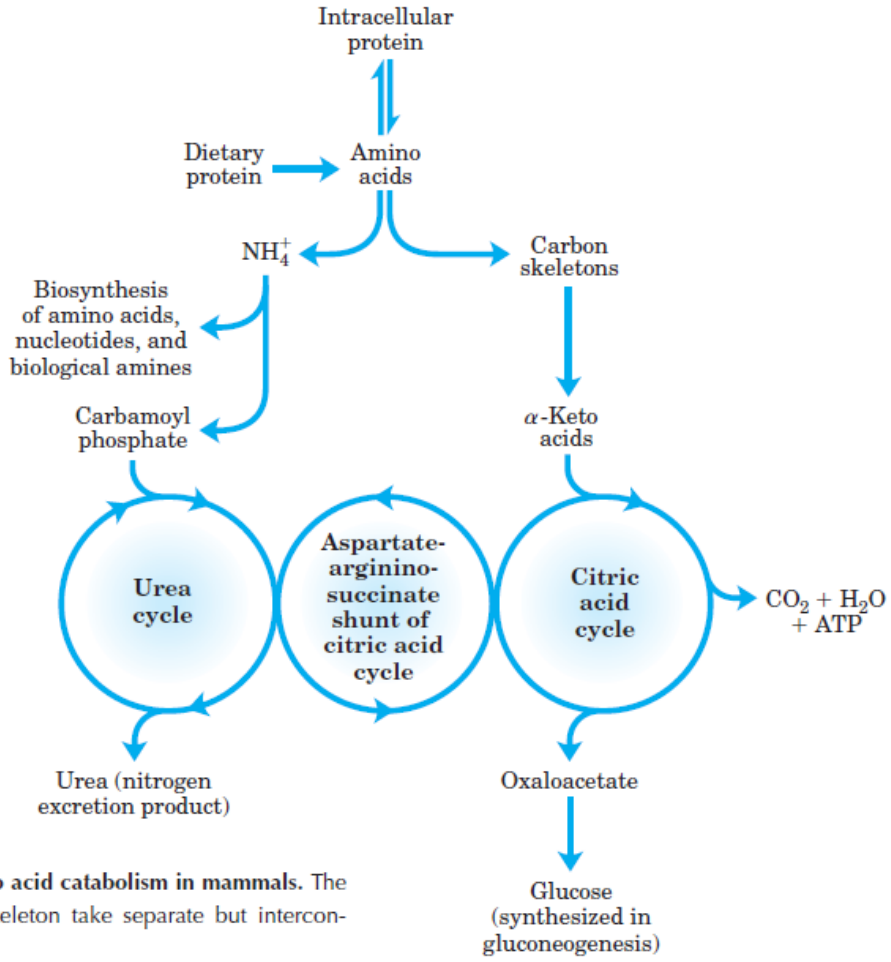


**FIGURE 18–1 Overview of amino acid catabolism in mammals.** The amino groups and the carbon skeleton take separate but interconnected pathways.

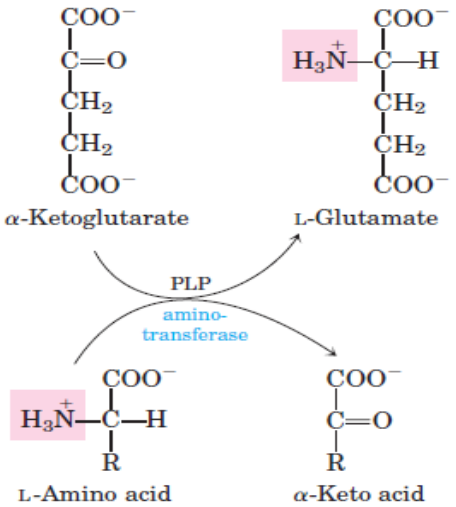


**FIGURE 18–4 Enzyme-catalyzed transaminations.** In many aminotransferase reactions, α-ketoglutarate is the amino group acceptor. All aminotransferases have pyridoxal phosphate (PLP) as cofactor. Although the reaction is shown here in the direction of transfer of the amino group to α-ketoglutarate, it is readily reversible.

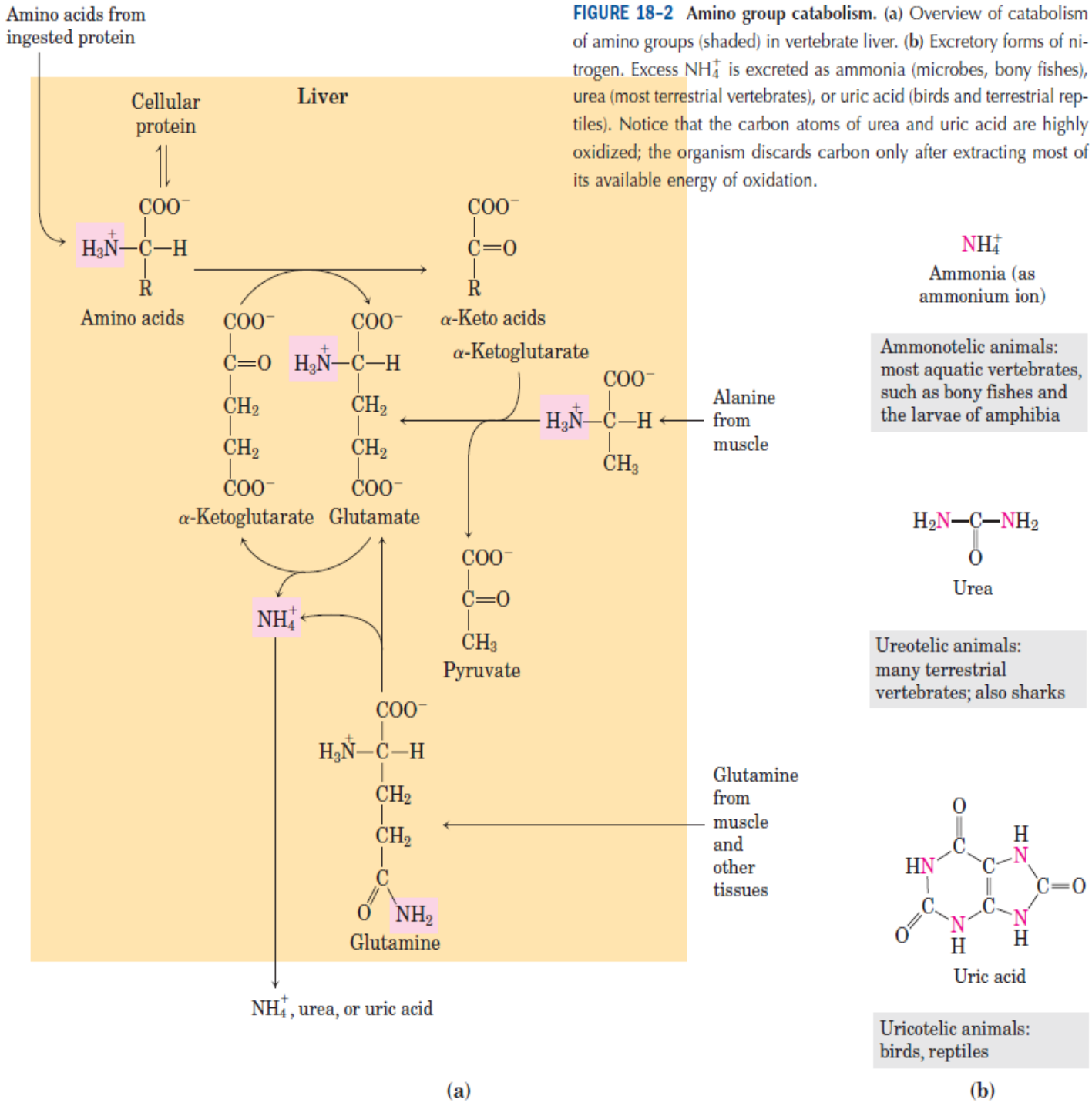


**FIGURE 18–2 Amino group catabolism.** (a) Overview of catabolism of amino groups (shaded) in vertebrate liver. (b) Excretory forms of nitrogen. Excess $NH_4^+$ is excreted as ammonia (microbes, bony fishes), urea (most terrestrial vertebrates), or uric acid (birds and terrestrial reptiles). Notice that the carbon atoms of urea and uric acid are highly oxidized; the organism discards carbon only after extracting most of its available energy of oxidation.

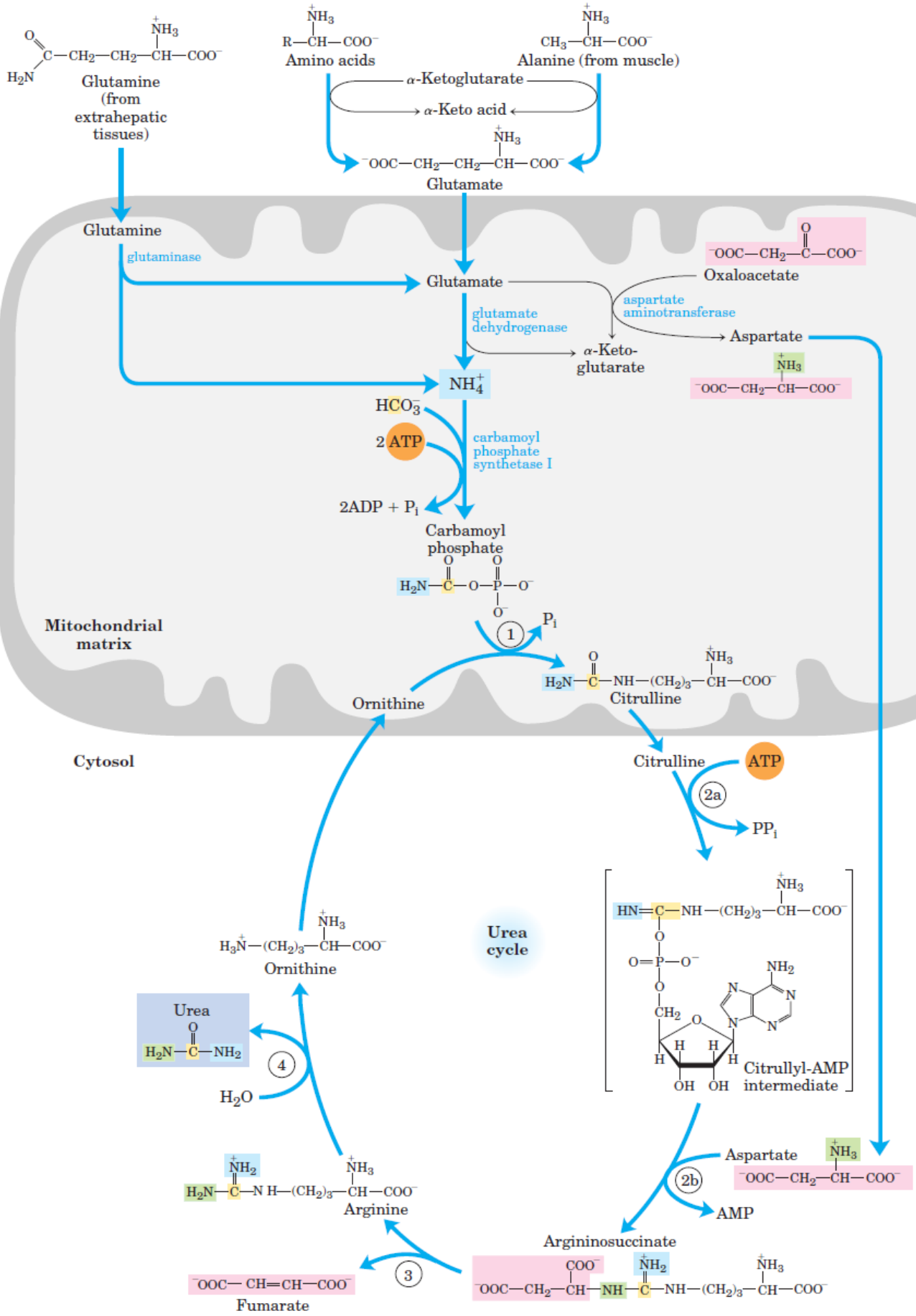
Glutamine (from extrahepatic tissues)
Amino acids
Alanine (from muscle)
α-Ketoglutarate
α-Keto acid
Glutamate
Glutamine
glutaminase
Glutamate
Oxaloacetate
aspartate aminotransferase
Aspartate
glutamate dehydrogenase
α-Keto-glutarate
NH4+
HCO3−
2 ATP
carbamoyl phosphate synthetase I
2ADP + Pi
Carbamoyl phosphate
Mitochondrial matrix
1
Pi
Ornithine
Citrulline
Cytosol
Citrulline
ATP
2a
PPi
Urea cycle
Citrullyl-AMP intermediate
Ornithine
Urea
4
H2O
Aspartate
2b
AMP
Argininosuccinate
Arginine
3
Fumarate

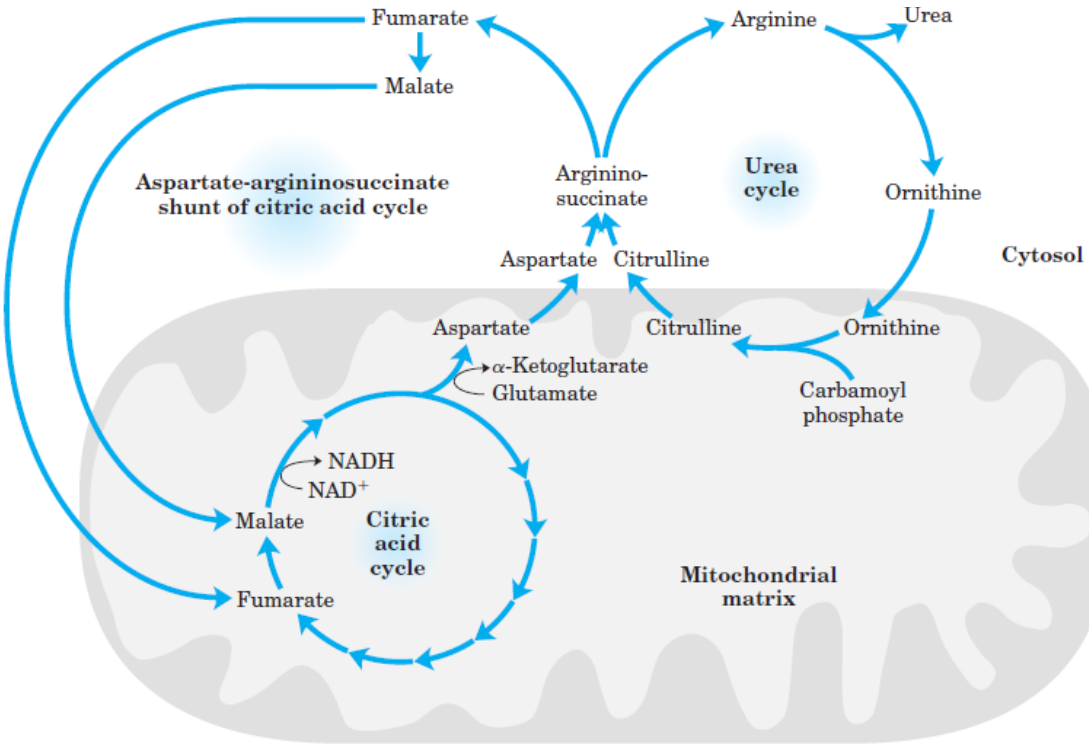


**FIGURE 18–12** **Links between the urea cycle and citric acid cycle.** The interconnected cycles have been called the "Krebs bicycle." The pathways linking the citric acid and urea cycles are called the aspartate-argininosuccinate shunt; these effectively link the fates of the amino groups and the carbon skeletons of amino acids. The interconnections are even more elaborate than the arrows suggest. For example, some citric acid cycle enzymes, such as fumarase and malate dehydrogenase, have both cytosolic and mitochondrial isozymes. Fumarate produced in the cytosol—whether by the urea cycle, purine biosynthesis, or other processes—can be converted to cytosolic malate, which is used in the cytosol or transported into mitochondria (via the malate-aspartate shuttle; see Fig. 19–27) to enter the citric acid cycle.

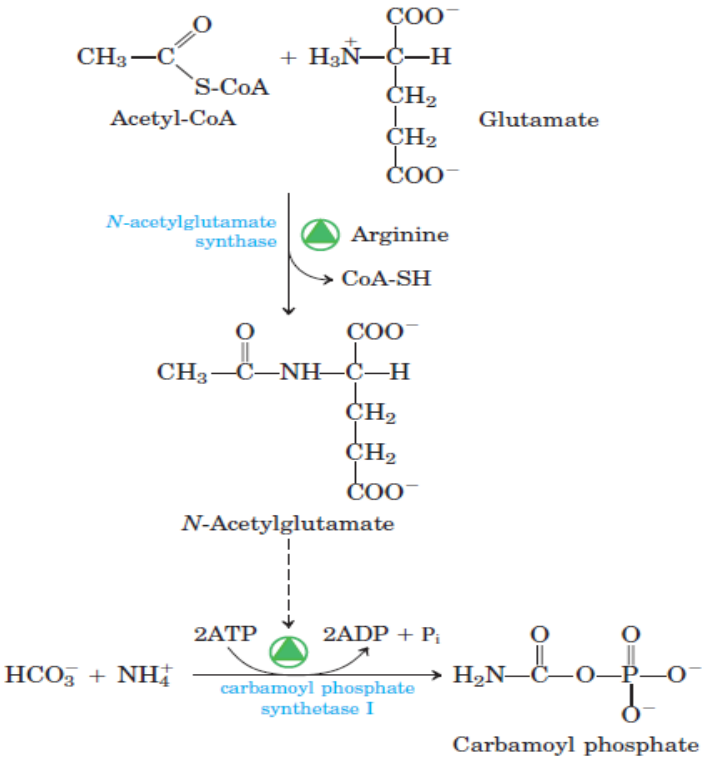


**FIGURE 18–13** **Synthesis of *N*-acetylglutamate and its activation of carbamoyl phosphate synthetase I.**

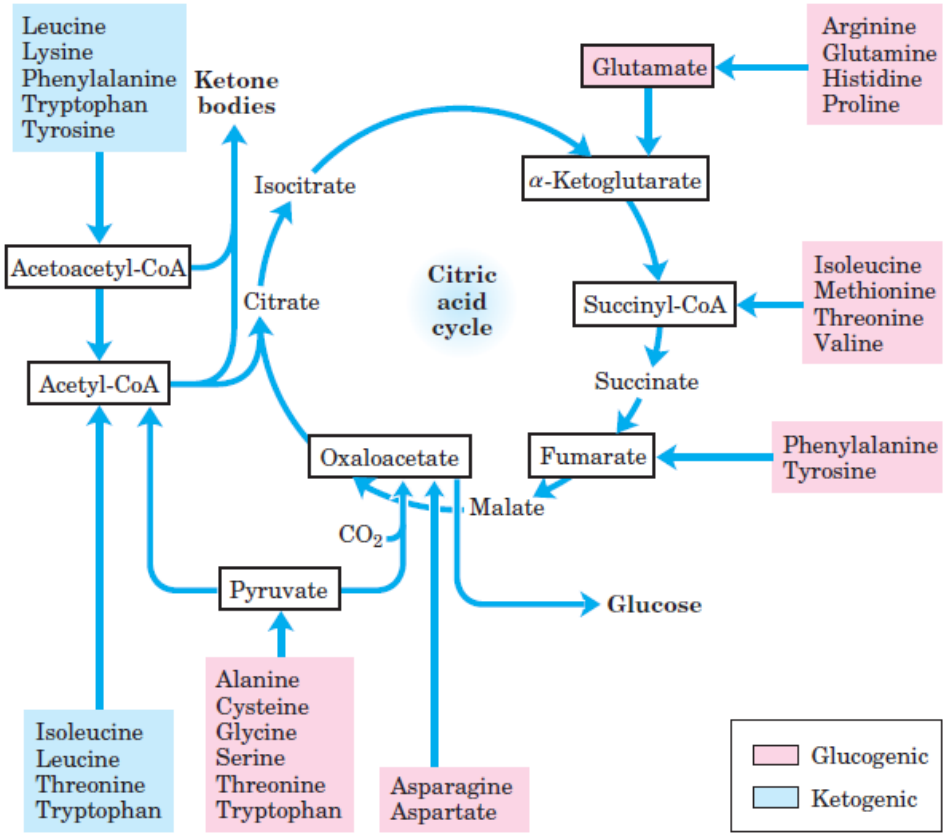


**FIGURE 18–15 Summary of amino acid catabolism.** Amino acids are grouped according to their major degradative end product. Some amino acids are listed more than once because different parts of their carbon skeletons are degraded to different end products. The figure shows the most important catabolic pathways in vertebrates, but there are minor variations among vertebrate species. Threonine, for instance, is degraded via at least two different pathways (see Figs 18–19, 18–27), and the importance of a given pathway can vary with the organism and its metabolic conditions. The glucogenic and ketogenic amino acids are also delineated in the figure, by color shading. Notice that five of the amino acids are both glucogenic and ketogenic. The amino acids degraded to pyruvate are also potentially ketogenic. Only two amino acids, leucine and lysine, are exclusively ketogenic.

**TABLE 18–1 Nonessential and Essential Amino Acids for Humans and the Albino Rat**

| *Nonessential* | *Conditionally essential** | *Essential* |
|---|---|---|
| Alanine | Arginine | Histidine |
| Asparagine | Cysteine | Isoleucine |
| Aspartate | Glutamine | Leucine |
| Glutamate | Glycine | Lysine |
| Serine | Proline | Methionine |
| | Tyrosine | Phenylalanine |
| | | Threonine |
| | | Tryptophan |
| | | Valine |

جلسه یازدهم: آنابولیسم اسید های آمینه و مشتقات آمینو اسید ها

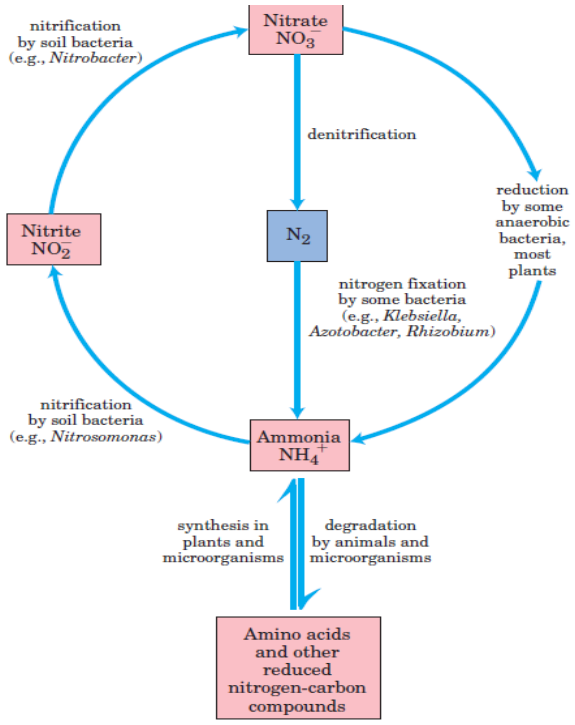


**FIGURE 22–1** The nitrogen cycle. The total amount of nitrogen fixed annually in the biosphere exceeds $10^{11}$ kg.

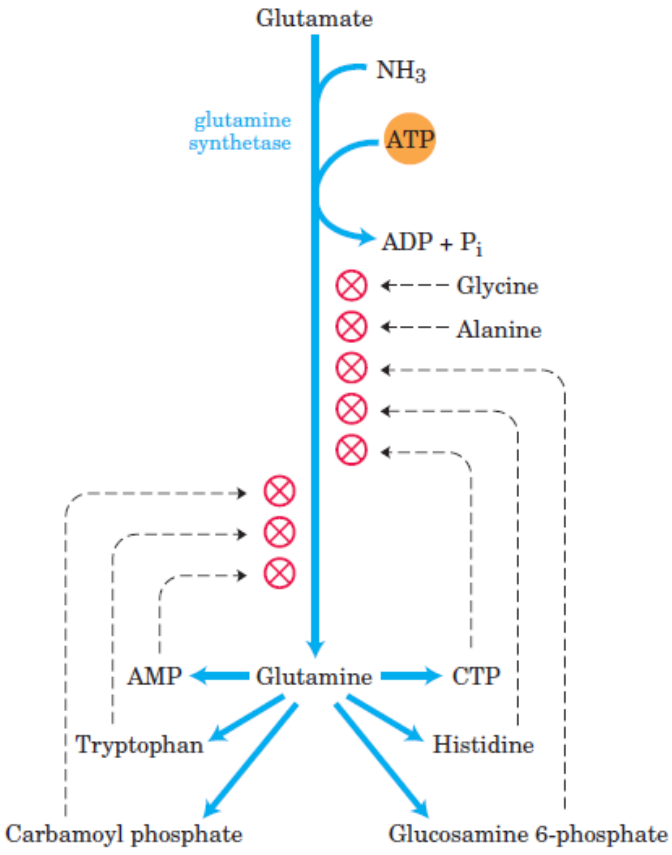


**TABLE 22–1** Amino Acid Biosynthetic Families, Grouped by Metabolic Precursor

**α-Ketoglutarate**
Glutamate
Glutamine
Proline
Arginine

**3-Phosphoglycerate**
Serine
Glycine
Cysteine

**Oxaloacetate**
Aspartate
Asparagine
Methionine*
Threonine*
Lysine*

**Pyruvate**
Alanine
Valine*
Leucine*
Isoleucine*

**Phosphoenolpyruvate and erythrose 4-phosphate**
Tryptophan*
Phenylalanine*
Tyrosine†

**Ribose 5-phosphate**
Histidine*

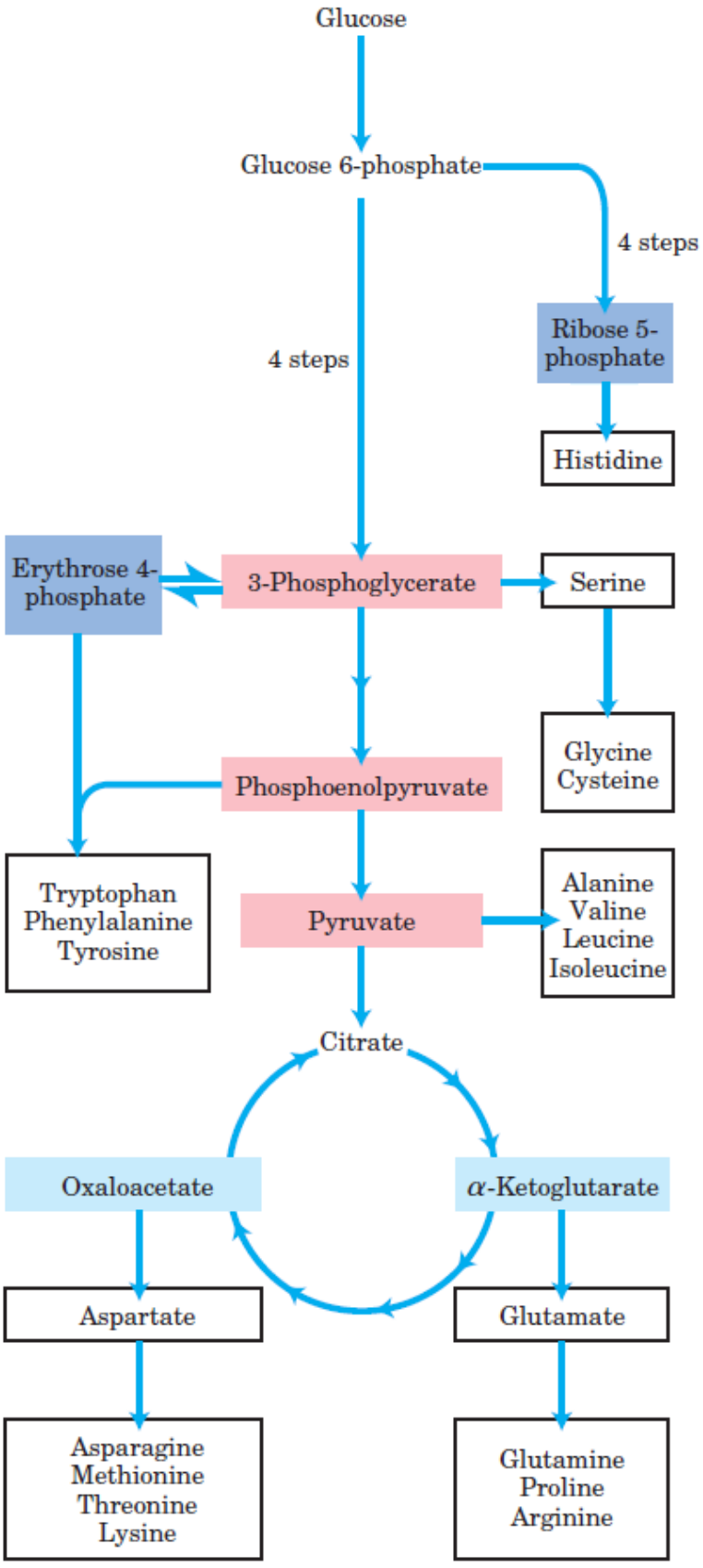


**FIGURE 22–9 Overview of amino acid biosynthesis.** The carbon skeleton precursors derive from three sources: glycolysis (pink), the citric acid cycle (blue), and the pentose phosphate pathway (purple).

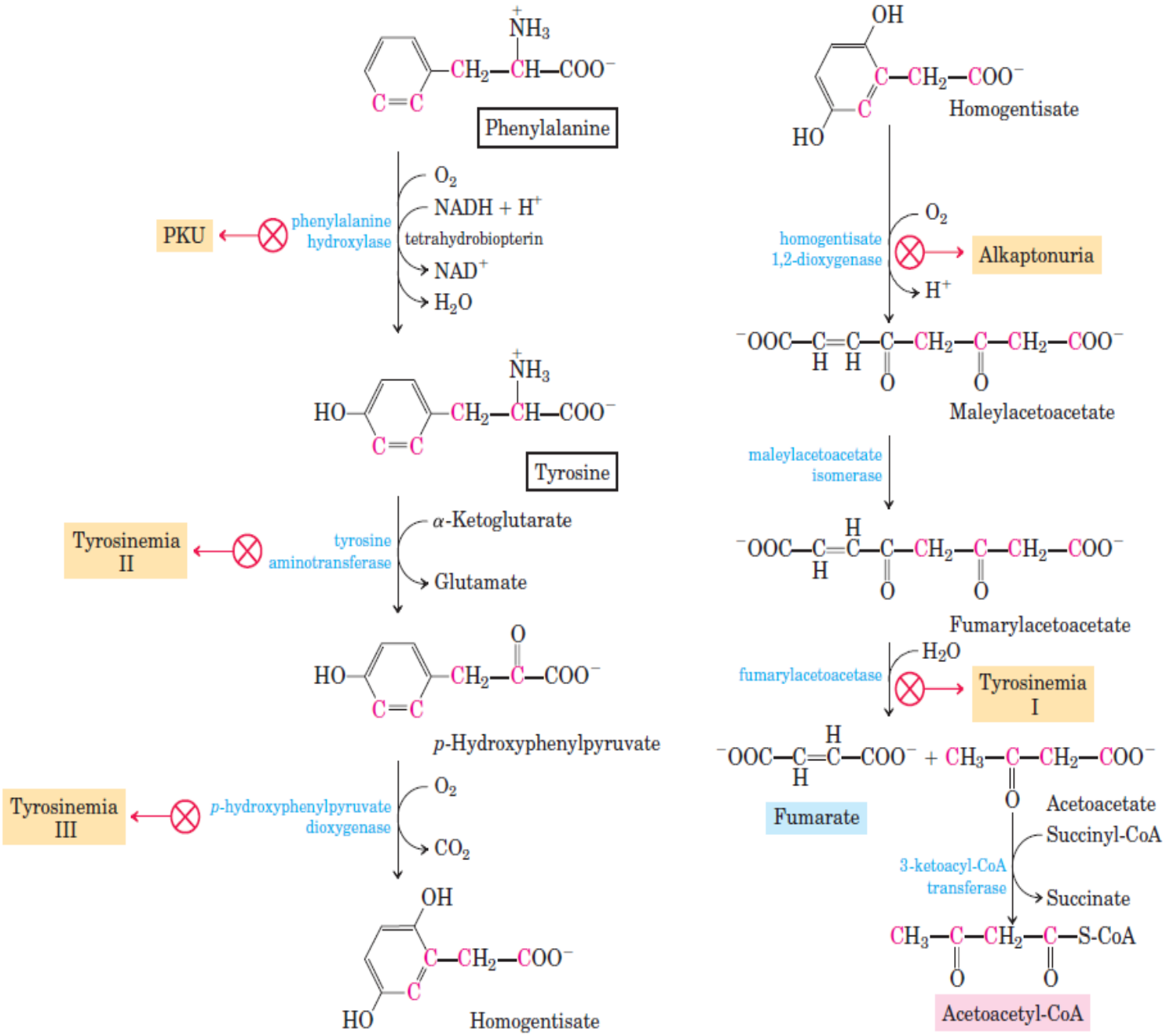


**FIGURE 18–23 Catabolic pathways for phenylalanine and tyrosine.** In humans these amino acids are normally converted to acetoacetyl-CoA and fumarate. Genetic defects in many of these enzymes cause inheritable human diseases (shaded yellow).

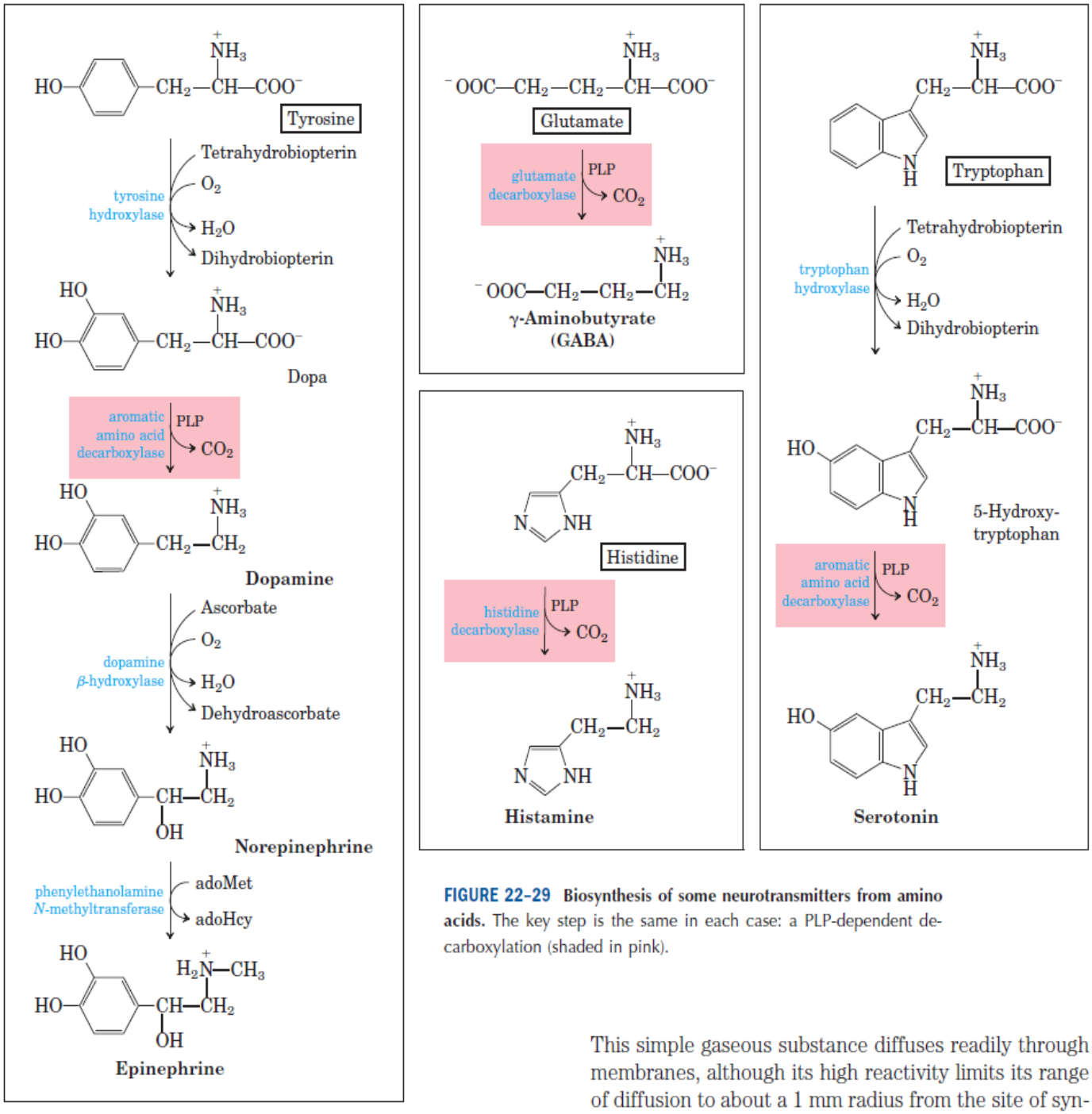


**FIGURE 22-29 Biosynthesis of some neurotransmitters from amino acids.** The key step is the same in each case: a PLP-dependent decarboxylation (shaded in pink).

This simple gaseous substance diffuses readily through membranes, although its high reactivity limits its range of diffusion to about a 1 mm radius from the site of syn-

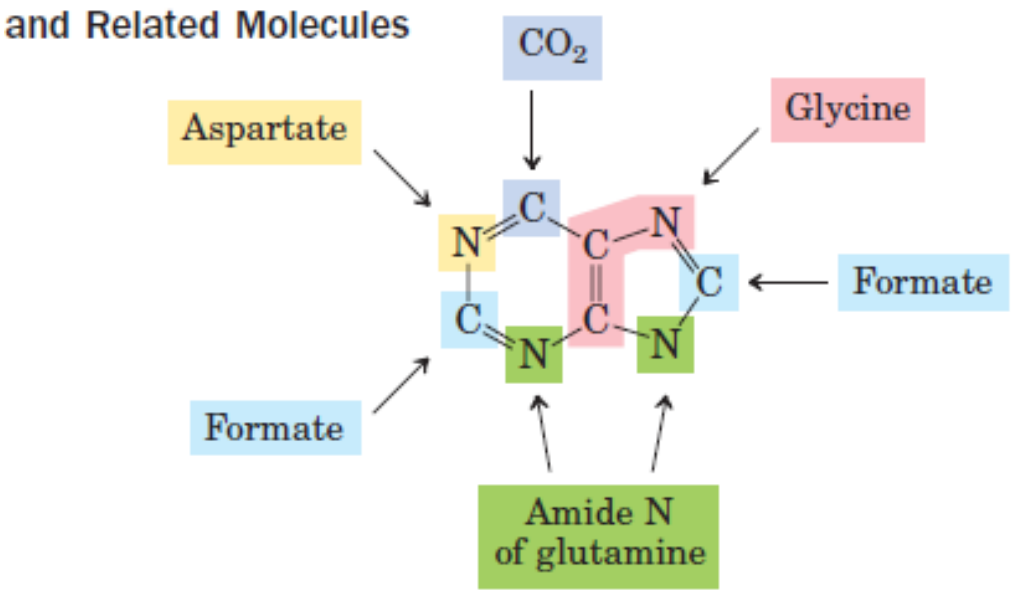


**FIGURE 22-32 Origin of the ring atoms of purines.** This information was obtained from isotopic experiments with $^{14}C$- or $^{15}N$-labeled precursors. Formate is supplied in the form of $N^{10}$-formyltetrahydrofolate.

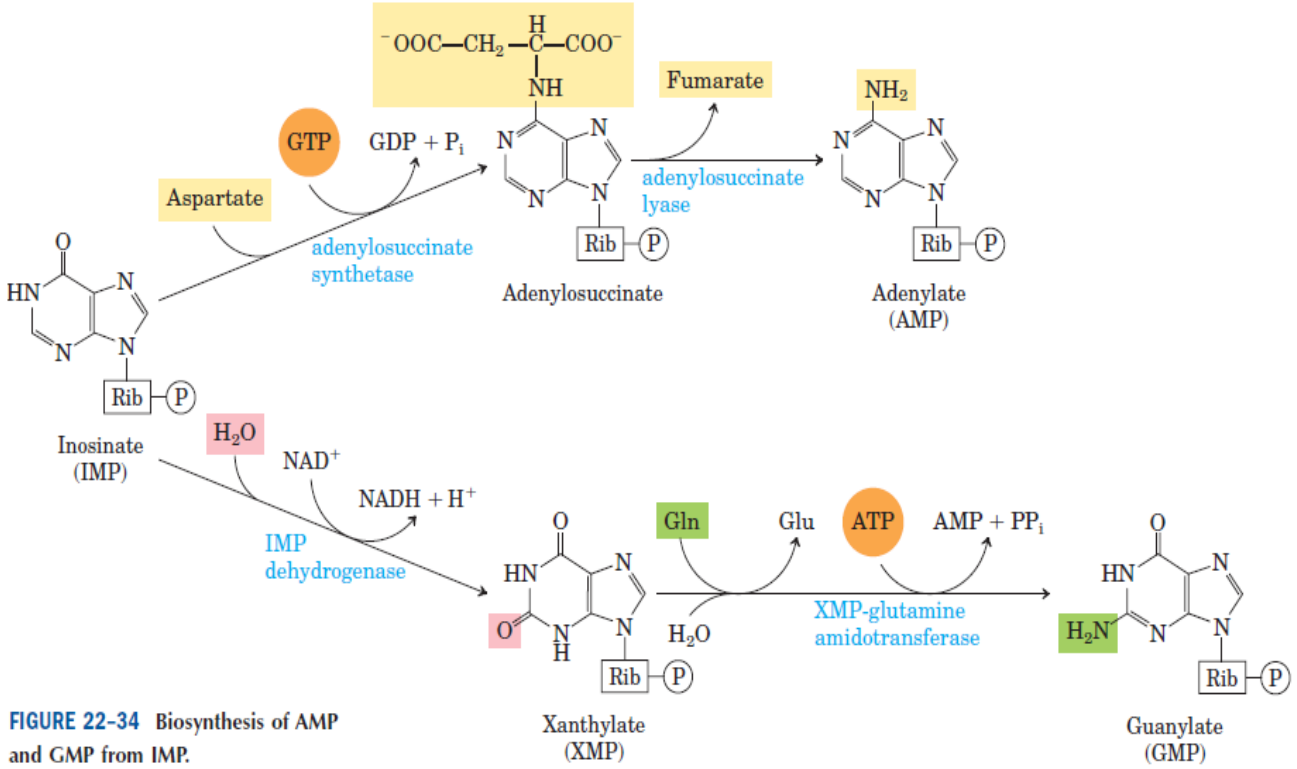


**FIGURE 22-34** Biosynthesis of AMP and GMP from IMP.

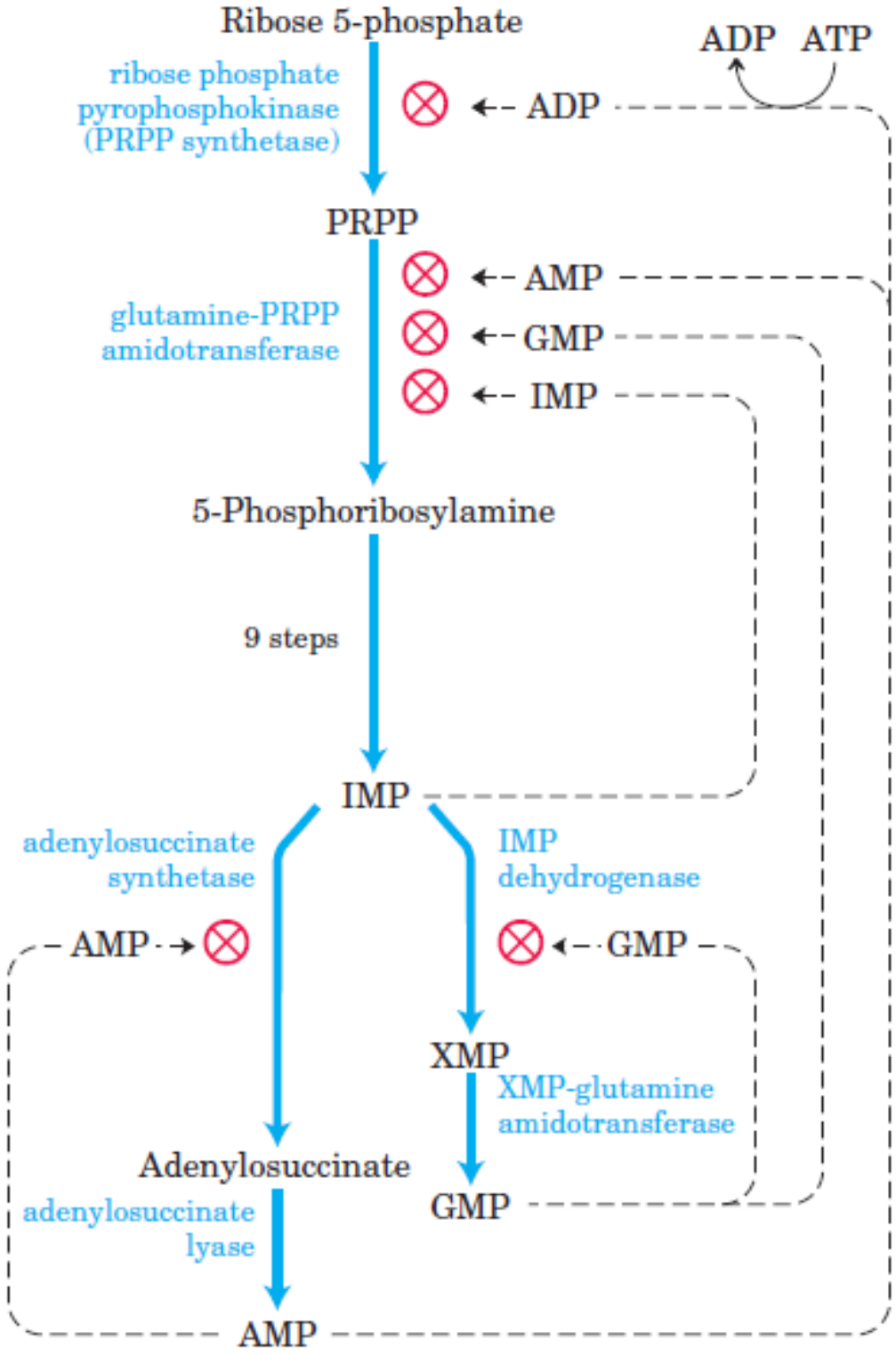


**FIGURE 22–35 Regulatory mechanisms in the biosynthesis of adenine and guanine nucleotides in *E. coli*.** Regulation of these pathways differs in other organisms.

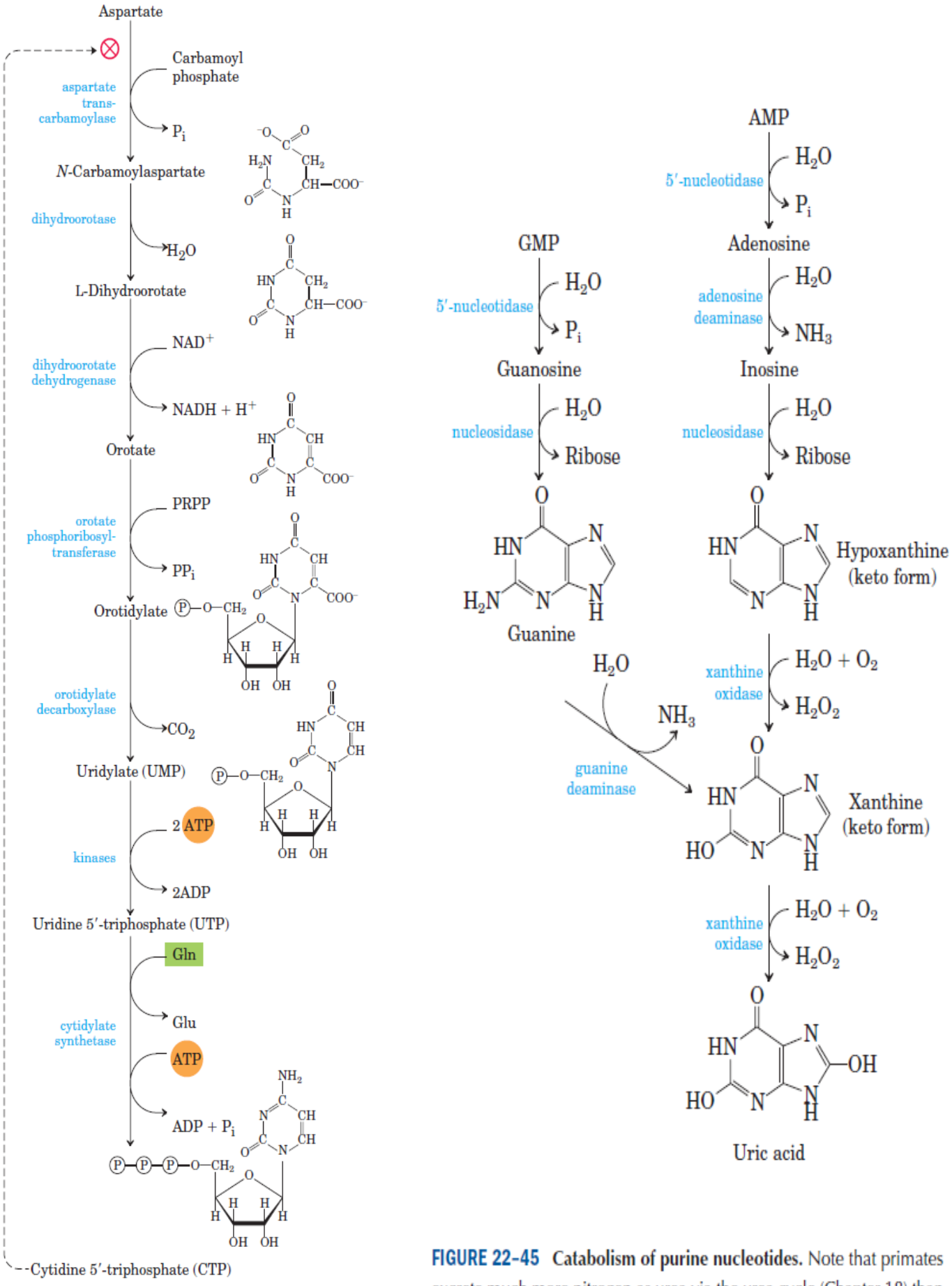


**FIGURE 22-45** **Catabolism of purine nucleotides.** Note that primates excrete much more nitrogen as urea via the urea cycle (Chapter 18) than